

SIMULATION, PERFORMANCE ANALYSIS AND IMPROVEMENTS OF SOLAR FARM INSTALLATION IN TANZANIA

Mohammed M. Haji

**A Dissertation Submitted in Partial Fulfilment of the Requirements for the Degree of
Master's in Sustainable Energy Science and Engineering of the Nelson Mandela African
Institution of Science and Technology**

Arusha, Tanzania

April, 2019

ABSTRACT

With the environmental advantages of solar energy, the use of solar photovoltaic (PV) in electricity generation is encouraged by Tanzanian governments, however, the number of institutions that are benefiting from installing grid-connected PV system and the electricity being generated are not clearly documented. Thus, in this study simulation, performance analysis and improvements of grid connected and standby PV system at Karume Institute of Science and Technology (KIST, Zanzibar) as well as Nelson Mandela African Institution of Science and Technology NM-AIST, Arusha) have been carried out. The analysis utilizes the power load data from the two different locations in Tanzania. The data (current and voltages) were obtained using the data loggers and the outputs such as power and energy were calculated. In addition, HOMER (Hybrid Optimization Model for Electric Renewables) software developed by the National Renewable Energy Laboratory (NREL), Department of Energy, United States of America was used to design and evaluate technical-performance and financial- options for off-grid and on-grid power systems for remote, stand-alone and distributed generation applications.

Therefore, in this study, the distance from the roof to the panel, reflection and inclination angles were observed to have significant impact on the performance of PV panels. High performance was recorded when the distance from the roof to the panel was 20 cm and the reflection and inclination angles were

45° and 20° respectively at KIST. The spacing provided good natural cooling of the panel while at the optimal reflection and inclination angles the solar intensity was improved due to the decreased angle of incidence. Additionally, the HOMER simulated results indicated that PV and grid combination at KIST exhibited the saving of 39.8% of the total energy consumption per day as compared to when only grid power is used, the cost of energy was reduced from \$0.1877 to \$0.113. In the other hand, the combination of grid, battery and PV systems at NM-AIST recorded the saving of 50.5% of energy usage per day, the cost of energy was reduced from \$0.22 849 to \$0.113.

DECLARATION

I, Mohammed M. Haji, declare that this dissertation is my own work and that it has not been presented and will not be presented to any other University for a similar or any other degree award.

Mohammed M. Haji

Name and signature of candidate

.....

Date

The above declaration is confirmed

Prof. Eugene Park

Name and signature of supervisor (1)

.....

Date

Dr. Thomas Kivevele

Name and signature of supervisor (2)

.....

Date

ACKNOWLEDGEMENTS

Writing this thesis has never been an easy task. Its completion is a result of a collective work; as many parties were involved in contributing and supporting this project. I would like to thank God for always being there for me and guiding me throughout. His love has been awesome for me throughout this long, tough and traumatic journey. I would like to express my earnest gratitude to my supervisors Prof. Eugene Park and Dr. Thomas Kivevele for their great support and supervision they gave me throughout to the completion of this study. Their reviews, comments, support, love and encouragement were really important, impressive and were immensely felt throughout. “Thank you” may not be enough to express my appreciation for your tireless kindness and support. So, in the lack of better words; I say thank you and God bless you.

To my family, I thank you for your amazing support during the whole process of my education.

DEDICATION

I dedicate this work to God Almighty my creator, my strong pillar, my source of inspiration, wisdom, knowledge and understanding. He has been the source of my strength throughout this program and on his wings only have I soared. I also dedicate this work to my first born; Naila Mohammed and the rest of my family members who has encourage me all the way and whose encouragement has made sure that I give it all it takes to finish that which I have started. To the whole community members who have been affected in every way possible by this quest. Thank you. My love for you all can never be quantified. God bless you.

Prof. Eugene Park

Name and signature of supervisor (1)

.....

Date

Dr. Thomas Kivevele

Name and signature of supervisor (2)

.....

Date

COPYRIGHT

All rights reserved. No part of this research report may be produced, stored in any retrieval system or transmitted in any form or by any means without a prior permission of the author or The Nelson Mandela African Institution of Science and Technology- Arusha, Tanzania on behalf.

CERTIFICATION

The undersigned certify that they have read and hereby recommend for examination of a dissertation entitled, “Simulation, performance analysis and improvements of solar farm installation in Tanzania” to be accepted in partial fulfillment of the requirements for the Degree of Master of Science in Renewable Energy Science and Engineering (Sustainable Energy Science and Engineering) of the Nelson Mandela African Institution of Science and Technology, Arusha, Tanzania.

.....

Prof. Eugene Park

.....

Date

.....

Dr. Thomas Kivevele

.....

Date

TABLE OF CONTENTS

ABSTRACT.....	i
DECLARATION	ii
ACKNOWLEDGEMENTS.....	iii
DEDICATION.....	iv
COPYRIGHT.....	v
CERTIFICATION	vi
TABLE OF CONTENTS.....	vii
LIST OF TABLES	x
LIST OF FIGURES	xi
LIST OF APPENDICES.....	xiii
LIST OF ABBREVIATIONS AND SYMBOLS	xiv
CHAPTER ONE	1
INTRODUCTION	1
1.1 Background Information.....	1
1.2 Solar Electricity in Tanzania.....	1
1.3 Research Problem and Justification	2
1.4 Objectives	2
1.4.1 General Objective	2
1.4.2 Specific Objectives	2
1.5 Research Questions.....	2
1.6 Significance of the Research.....	3
1.7 Scope of the Study	3
CHAPTER TWO	4
LITERATURE REVIEW	4
2.1 Grid connected PV system.....	4
2.2 Challenges of Solar Electricity	5

2.3 The HOMER Software	6
2.4 Application of HOMER on Solar Photovoltaic	10
CHAPTER THREE	11
MATERIALS AND METHODS.....	11
3.1 Study Locations	11
3.2 Instruments.....	11
3.3 Technical Data	11
3.4 Site location and Systems specific information	12
3.5 Current and Voltage Measurements (D.C Measurements)	13
3.6 The Grid Connected PV System at KIST and NM-AIST	14
3.7 Performance Parameters	16
3.8 Simulation using HOMER Software	19
CHAPTER FOUR.....	24
RESULTS AND DISCUSSION	24
4.1 Performance Investigation at KIST	24
4.1.1 Impact of Distance from the Roof	24
4.1.2 Impact of Reflector	24
4.1.3 Impact of Angle of Inclination.....	25
4.2 Grid-Tied Parameters Analysis at KIST	25
4.2.1 Direct Current Energy Produced and Alternating Current Energy Injected to Grid	26
4.2.2 Power Input to Inverter and Power Output from Inverter.....	26
4.2.3 Grid connected results at KIST	29
4.3 Grid Connected PV System at NM-AIST.....	29
4.3.1 Power vs Total voltage and Power vs Current.....	29
4.3.2 South facing Panels Current vs Voltage and North facing Current vs Voltage.....	30
4.3.3 North facing Panels Voltage vs Currents and South facing Panels Voltage vs Currents.....	31
4.4 HOMER Simulation.....	31

4.4.1 KIST Simulation Results	31
4.4.2 Cash Summary (Annualized and Net Present).....	32
4.4.3 Cash Summary (Annualized and Net Present) at KIST	34
4.4.4 Profile Time Series	35
4.4.5 Electrical Simulation.....	35
4.4.6 PV Simulation at KIST	36
4.4.7 Emissions Results for KIST	37
4.5 NM-AIST Simulation Results	37
4.5.1 Cash Summary (Annualized and Net Present) at NM-AIST	38
4.5.2 Cash Summary (Annualized by Cost Type) at NM-AIST	39
4.5.3 Electrical Simulation at NM-AIST	40
4.5.4 PV Simulation at NM-AIST	41
4.5.5 Batteries Simulation at NM-AIST	41
4.5.6 Grid Simulation at NM-AIST	42
4.5.7 Emissions Results for NM-AIST	43
4.5.8 Daily Load (July 2017)	43
4.5.9 Total Renewable Power Output	43
CHAPTER FIVE	45
CONCLUSION AND RECOMMENDATIONS	45
5.1 Conclusion	45
5.2 Recommendations.....	45
REFERENCES	47
APPENDICES	50
RESEARCH OUTPUTS.....	52
Output 1: Paper Presentation	52
Output 2: Poster presentation.....	64

LIST OF TABLES

Table 1: Technical detail of the systems.....	12
Table 2: Systems specific information.....	12
Table 3: Specification of solar panel	13
Table 4: Systems input data	21
Table 6: System configuration inputs	22
Table 7: Systems converter costs and inputs	22
Table 8: Systems battery costs and specification.....	23
Table 9: Economics, system control, emission and constraints.....	44

LIST OF FIGURES

Figure 1: KIST PV System arrangement	13
Figure 2: Installed rooftop solar PV at KIST	14
Figure 3: Installed rooftop solar PV at NM-AIST	14
Figure 4: Block diagram of grid connected KIST-PV system	15
Figure 5: NM-AIST PV System arrangement	15
Figure 6: I-V Characteristics.....	17
Figure 7: Systems configuration (a) KIST and (b) NM-AIST	19
Figure 9: Systems solar insolation	22
Figure 10: Impact of distance from the roof to output power.....	24
Figure 11: Impact of different inclination for the reflector to output power	25
Figure 12: Impact of angle of inclination to output power	25
Figure 13: Energy in Watt-hour (a) D.C Energy produced (b) A.C Energy injected	26
Figure 14: Power in Watts (a) Input to inverter (b) Output from inverter	27
Figure 15: Yield ratios (a) Array yield (b) Final yield.....	27
Figure 16: Efficiencies (a) System (b) Inverter	28
Figure 17: PV observation (a) On load efficiency (b) Performance ratio.....	28
Figure 18: Factors for the PV module (a) Capacity factor (b) Temperature	28
Figure 19: Battery voltages	29
Figure 20: Power characteristics (a) Power vs total voltage (b) Power vs current	30
Figure 21: Panel facing current vs voltage (a) South facing (b) North facing.....	30
Figure 22: Current vs panel facing voltage (a) Current vs north facing voltage (b) Current vs south facing voltage	31
Figure 23: Simulation results for KIST	32
Figure 24: Cash summary (Annually by component) results for KIST	33
Figure 25: Cash summary (Net Present by component) results for KIST	33

Figure 26: Cash summary (Annualized by cost type) results for KIST	34
Figure 27: Cash summary (Net Present by cost type) results for KIST	34
Figure 28: Profile time series results for KIST	35
Figure 29: Electrical simulation results for KIST	36
Figure 30: PV simulation results for KIST	36
Figure 31: Emissions results for KIST	37
Figure 32: Simulation results for NM-AIST	38
Figure 33: Cost summary (Net present by component) results for NM-AIST	38
Figure 34: Cost summary (Annualized by component) results for NM-AIST	39
Figure 35: Cost summary (Net present by cost type) results for NM-AIST	39
Figure 36: Cost summary (Annualized by cost type) results for NM-AIST	40
Figure 37: Electrical results for NM-AIST	40
Figure 38: PV results for NM-AIST	41
Figure 39: Batteries simulation results for NM-AIST	42
Figure 40: Grid simulation results for NM-AIST	42
Figure 41: Emissions results for NM-AIST	43
Figure 42: July 2017 load curves results for NM-AIST	43
Figure 43: Hourly renewable power output results for NM-AIST	43

LIST OF APPENDICES

Appendix 1: Standalone measurement for solar PV in KIST	50
Appendix 2: Grid connected measurement parameters at KIST	51

LIST OF ABBREVIATIONS AND SYMBOLS

DC	Direct current
AC	Alternating current
STC	Standard Test Conditions
NOCT	Normal Operating Cell Temperature
TANESCO	Tanzania Electric Supply Company Limited
ZECO	Zanzibar Electricity Corporation
I_{sc}	Short circuit current
V_{oc}	Open circuit voltage
W_p	Peak output power
I	Electrical Current
V	Voltage/Volts
P	Power
A	Amperes
W	Watts
KIST	Karume Institute of Science and Technology
HOMER	Hybrid Optimization Model for Electric Renewables
PV	Photovoltaic
IEC	International Electrotechnical Commission
NM-AIST	The Nelson Mandela African Institution of Science and Technology

CHAPTER ONE

INTRODUCTION

1.1 Background Information

In sub-Saharan Africa (SSA), about 75% of the populations do not have electricity access and rely on non-renewable energy sources mainly fossil fuels and wood fuel for energy (Mohammed *et al.*, 2013). The reliance on fossil fuels energy is too costly in addition to contributing to greenhouse gas emissions, which paradoxically limits socio-economic advancement for over 600 million people in SSA, - who live in extreme poverty and already lack proper health care, education, business opportunities (Herscowitz and Pielli, 2016). Therefore, renewable energy sources such as solar energy wind energy, hydroelectricity etc., are, thus considered the best alternative energy sources because they do not pollute the environment, emit no greenhouse gases (e.g. carbon dioxide, nitrous oxides, methane etc.) which increase greenhouse effect that drive global warming and climate change.

Tanzania, for instance - like many Sub Saharan Africa (SSA) countries, most parts of the country still suffer from the lack of adequate, reliable, effective and sufficient electricity. The rural areas and other remote locations which are off-grid are the most affected. Thus, Tanzania with total area of 945 000 km², only 2605 km² was covered national grid by 2000 and was served by 132 kV and 220 kV transmission networks (Gwang'ombe and Mwiha, 2005). The available energy sources in Tanzania include hydroelectricity, coal, natural gas, solar, biomass and imported petroleum.

1.2 Solar Electricity in Tanzania

There is a high potential for using solar electricity as a major renewable energy source in Tanzania if scaled up, and will also serve to offset the anthropogenic greenhouse gas emissions from fossil energy sources. This is because solar energy is the most readily available renewable source of energy across Tanzania and is free, hence it has high potential to contribute towards sustainable energy development strategies in the country. Besides, solar energy is non-polluting and maintenance free. It is against this background that, solar energy is becoming more and more attractive in the developing economies, especially with the escalating fluctuations and inadequate supply of grid power (Cogeneration *et al.*, 2004).

1.3 Research Problem and Justification

The major limitation of solar electricity supply is the technical capacity and guidelines mainly in systems installation onsite, - which affects performance of the systems. The choice of system components suitable for different locations, buildings and landscape orientations is critical, especially when it comes to PV systems in sub-optimal locations such as west-facing roofs or flat roofs where mounting the modules is not an option because of load limitations. Taking into account the latest innovations is critical, e.g. specialized products targeted for north - south facing roofs, light-weight flexible PV modules etc.

Consequently, most of the common errors or mistakes are often made at the installation stage including incorrect energy yield prediction, different azimuths or inclinations in the same string with modules of different power rating, insufficient structural load calculations, cable sizing, and inverter mismatch. Therefore, it is clear that any last-minute changes in one of the design stages affects the entire configuration of the PV system design and can have a detrimental impact on the performance or safety of the final installation. Therefore, this study, aims to document standard procedures and facilitate proper PV installation and uptake in Tanzania to improve reliability, stability and efficiency of the PV installation using academic institutions as a case study.

1.4 Objectives

1.4.1 General Objective

The general objective of the present study is to investigate the performance of solar farms installation in Tanzania through experiments and simulations.

1.4.2 Specific Objectives

The specific objectives were:

- (i) To investigate the performance of installed solar farms at KIST and NM-AIST.
- (ii) To evaluate the improvements of solar panels installation.
- (iii) To simulate grid and non-grid connected solar farms using HOMER software at KIST and NM-AIST.

1.5 Research Questions

This research intended to answer the following:

- (i) What is the performance of solar farms installed at KIST and NM-AIST?

- (ii) What are the effects influencing the performance of solar panels?
- (iii) What is the best hybrid configuration for grid and non-grid connected solar farms?

1.6 Significance of the Research

Solar energy can play a major role in sustainable development especially achieving Sustainable Development Goal no. 7 which is about ensuring access to affordable, reliable, sustainable and modern energy for all (Bank, 2015). Access to affordable, reliable and sustainable energy is crucial to achieving many of the Sustainable Development Goals (SDGs), from poverty eradication via advancements in health, education, water supply and industrialization to mitigating climate change. Energy access, however, varies widely across countries and the current rate of progress falls short of what will be required to achieve the goal.

Henceforth, proper installation of solar systems not only will help reduce fossil fuel energy usage and boost performance but also create a more robust or reliable renewable energy alternative across Tanzania. One potential scaling approach identified is the use of solar electricity at institutions, which presents a good opportunity for hosting solar technologies. The institutions have increasing demand for reliable electricity supply systems due to their increasing population that raises the demand of electricity.

1.7 Scope of the Study

Achieving high performance in meeting service level agreement (SLA) it requires data monitoring and managing of power output and quality. The systematic monitoring of reliability statistics issues and root causes continually strive to improve the reliability of the electricity (Limmanee *et al.*, 2017).

Hence, this study outlines simulation, performance analysis and improvements of solar farms for delivering reliable power, safely and efficiently to the consumers for support system enabling real-time analysis. This will serve to provide greater transparency for operating and maintaining a plant by providing a means of improving the efficiency and productivity of PV performance.

CHAPTER TWO

LITERATURE REVIEW

2.1 Grid connected PV system

The grid connected PV system is the electric power generated by solar PV power system that is connected to the utility grid. The current and voltage values are then injected into the grid.

The main component for grid-connected solar PV systems comprise of the following:

- (i) Solar PV modules connected in series and parallel, - depending on the solar PV array size to generate DC power directly from the sun's interrupted solar power,
- (ii) Solar charger controller making sure the solar PV modules generated DC power at their best power output at any given time during sunshine hours,
- (iii) Grid-connected DC/AC inverter, making sure the generated and converted AC power is safely fed into the utility grid whenever the grid is available and connection safety equipment like DC/AC breakers fuses etc., according to the local utility's rules and regulations.

The process of converting light (photons) to electricity (voltage) is called the solar photovoltaic (PV) effect. Photovoltaic solar cells convert sunlight directly into solar power (electricity). When exposed to daylight, electrons in the semi-conducting material absorb the photons, causing them to become highly energized and move between the top and bottom surfaces of the semi-conducting material. This movement of electrons generates a current known as a direct current (DC). This is then fed through an inverter, which converts the power to alternating current (AC) then all the electricity produced by the solar panels is produced as direct current (DC), which differs from the electricity that is distributed through the grid and we use in our homes, which is alternating current (AC). For this reason, most solar photovoltaic systems are now connected up with some type of inverter, which changes the DC to AC, allowing the individual to sell the electricity back to the grid (in grid-tied systems) or to be used easily in homes.

Simulation and performance analysis requires a large quantity of input data like solar irradiation, local weather conditions and other technical parameters of the planned PV systems (Yang *et al.*, 2003). The grid-connected rooftop solar PV power systems generate DC power direct from the sun's intercepted solar energy through solar PV modules. The solar PV modules are connected through a solar charger controller, to a grid-inverter, converting the generated DC power into AC Power, feeding the converted AC power into the utility grid.

The grid tied systems allow taking advantage of the free electricity created from the solar PV system as well as the electric grid.

In case grid-connected PV systems do not have battery storage, the excess energy after supplying the primary load from the PV array can be sent to the utility grid. On the other hand, energy can be drawn from the grid when energy generated from PV is insufficient for the primary load. Therefore, the difference between price of buying electricity from the grid and that of selling to the grid from the PV system is a substantial factor in determining the optimal size of grid-connected PV systems (Ramli *et al.*, 2015).

This gives much more flexibility, since the much electricity at any time which supplies first the power demands of the institute the system is installed and selling the excess power to the local electricity provider (utility) at a defined feed-in tariff, paid by the utility company to the grid-connected solar PV system owner, due to generous government subsidies (guaranteed for 25 years from the date of installation). Additionally, they help to reduce reliance on the grid, and also reduce electricity bills.

2.2 Challenges of Solar Electricity

A solar power plant is based on the conversion of sunlight into electricity, either directly using photovoltaic (PV), or indirectly using concentrated solar power (Bull, 2001). Both the voltage and current are a function of light falling on solar PV. However, too much insolation on the cell causes saturation, and eventually reduces the power output due to the increase in mobility of electrons and temperature (Shukla *et al.*, 2016). Another challenge is tracking of the sun according to the PV module, thus orienting the panel in such a direction so that panel receives maximum irradiance. Therefore, successful integration of solar energy technologies into the existing energy structure depends on detailed knowledge of the solar resource availability at a particular location (Hammer *et al.*, 2003).

But due to evolution of technology, solar panels available today are smaller, more robust and more effective than ever before. Efficiency levels are improving, especially in poor light conditions and photovoltaic (PV) systems was experience an enormous increase in the decades.

2.3 The HOMER Software

Many researchers and engineers have argued and have presented different ideas on this topic using different software including Hybrid Optimization Model for Electric Renewables (HOMER) software but the performance and improvement on solar differ according to the location of the area and characteristics of the solar panel.

Ani and Abubakar (2015) did feasibility analysis and simulation of integrated renewable energy system for power generation: A hypothetical study of rural health clinic of Integrated Renewable Energy (IRE) using solar photovoltaic (PV) and wind turbine (WT) system in a hypothetical study of rural health clinic in Borno State, Nigeria. The simulation and optimization for the optimal integrated renewable energy system configuration consists of 5 kW PV array, 7.5 kW DC wind turbine, 24 unit Surrette 6CS25P battery cycle charging, and a 19 kW AC/DC converter. Photovoltaic power generated electricity 9138 kWh/year while the wind turbine system generated electricity 7490 kWh/year, giving the total electrical generation of the system as 16 628 kWh/year. This would be suitable for deployment of 100% clean energy for uninterruptable power performance in the health clinic. They conclude that, with a low energy health facility, it is possible to meet the entire annual energy demand of a health clinic solely through a stand-alone integrated renewable PV/wind energy supply.

Anwari *et al.* (2011) described and analyzed photovoltaic power system simulation for small industry area. The modeling and simulation of 1MW grid connected PV system was conducted using National Renewable Energy Laboratory's (NREL) HOMER software, and the optimum system was analyzed to see the economic feasibility of the system in a small industry area in Malacca, Malaysia. The system was expected to foresee reduced grid energy consumption. Emphasis was also placed on reduction of greenhouse gases emission. The HOMER software was therefore used to simulate the system and perform optimization according to the available usage data and the available renewable energy (sun radiation) data. In addition, the mechanism of switching the master function between the diesel generator and the PV array-inverter assembly in a stand-alone power system was also proposed and analyzed. Finally, some experimental results on a practical system were compared to the simulation results and confirmed the usefulness of the proposed approach to the development of renewable energy systems.

Mishra *et al.* (2016) reported the design and simulation of a solar–wind–biogas hybrid system architecture using HOMER in India. In rural areas, light is usually unavailable and if it does,

it is mostly an incandescent light used for household lighting instead of fluorescent. System reliability, economy and environmental issues are the three major issues for decentralized electrification. So, finding the best suited hybrid system configuration to overcome these constraints is the need of the hour. It is at this stage that HOMER comes into the picture and was realized that was useful for rural to urban applications however the PV characteristics are missing.

Bernal-Agustín and Dufo-Lopez (2009) presented the simulation and optimization of stand-alone hybrid renewable energy systems. The hybrid energy system comes from the biomass gasifier generator set, solar and fuel cell with battery storage system to fulfill partially load requirements. The computation software used for this work was HOMER Pro 3.2.3. HOMER Pro is a design simulation model that analyzed the sizing, costing optimization and control strategy of the hybrid energy system. The analysis of such hybrid energy systems feeding AC primary load of 101 kWh/day energy consumption with a 5 kW maximum load demand was conducted. Moreover, the control scheme is presented with capabilities of simultaneously and independently regulating both active and reactive power exchange with the electric grid. The simulation results showed that optimized size of components, biomass gasifier (5 kW), solar (5 kW) and fuel cell (5 kW), exhibited optimized cost of energy of about 15.064 Rs/kWh and the efficiency of the system was increased.

Shukla *et al.* (2016) focused on Simulation and performance analysis of 110 kWp grid-connected photovoltaic system for residential building in India: A comparative analysis of various PV technology possible variations of values of constants should be taken into account. The descriptions were on some characteristics of different types of batteries required for proposing a general model of the advanced based on the analysis, it was seen that both, the battery voltage and the current capable of being delivered at any given time, generally depends on several factors. Among the most important ones are the room temperature, the amount of charge/discharge cycles the battery has been subjected to (cycles), the depth of charge/discharge and the state of charge/discharge to observe its behavior in power quality or energy management events, this action sets a time within which the temperature can be considered constant for power quality-like events.

Ishaque *et al.* (2012) argued on parameter extraction of solar photovoltaic modules using penalty-based differential evolution using two diode model of a solar cell is used as the basis for the extraction problem. The performances are evaluated using the well-known quality test

and student *T*-tests. Furthermore, the P-DE extraction method is practically validated by six solar modules of different types (multi-crystalline, mono-crystalline, and thin-film) in predicting the performance of the solar system under partial shading conditions graphically but not simulated using software.

Parida *et al.* (2011) did a review of solar photovoltaic technologies concerning on global environmental and the escalating demand for energy, and examined that its power generating capability, the different existing light absorbing materials used, its environmental aspect coupled with a variety of its applications on the different existing performance and reliability evaluation models, sizing and control, grid connection and distribution effects the performance of the system.

Gupta and Srinivasa (2012) considered a design, simulation and verification of generalized Photovoltaic cells model using first principles modeling. The consideration implementation of a generalized photovoltaic model of PV cell, module, and array model applicable for mono crystalline, poly crystalline silicon, thin film like CIS, CdTe, Amorphous silicon, polymer from various manufacturers on simulation software platform using first principle method. This model is known to have better accuracy estimation of electrical behavior of the cell with respect to changes on environmental parameter of temperature and irradiance. All inputs to the model can be easily extracted from standard PV module datasheet. The functioning of the proposed model was evaluated by simulation. The accuracy of the simulation was verified by comparing output current and power characteristics of PV cell. Liu *et al.* (2012) did a research on techno-economic simulation and optimization of residential grid-connected PV system for the Queensland climate. The solar irradiation data of the 4 typical climate zones of Queensland, including tropical, sub-tropical, hot arid, and warm temperature zone, were investigated. Using global solar irradiation as solar energy resource data, the price of PV devices, batteries, converters, and grid electricity tariff and sale-back tariff as economic analysis inputs, the system was simulated and optimized by HOMER software. The optimized system not only satisfies the typical residential load of 23 kWh per day but also met the requirement of minimizing the total costs of system investment and electricity consumption during the system's lifetime. It was found that under the specific climatic conditions of the eleven main cities of Queensland, a PV system was an effective way to decrease electricity bills and mitigate carbon dioxide emission. In particular, a 6 kW PV system in Townsville was able to deal with 61% of the total electricity load and conserved

more than 90% of electricity payments and reduced approximately 95% of carbon dioxide emission. It was also found that for all the cities the systems with 20–25 degrees of slope had the best performance including the least cost of energy (COE) and the least carbon dioxide emission.

Bernal-Agustín and Dufo-Lopez (2009) reported optimization and simulation of solar photovoltaic cell using HOMER: A Case study of a residential building in Malviya Nagar, Jaipur (India) that had total roof area of 576 m² which comprises of 16 flat. The whole system of photovoltaic cell was optimized and simulated by using HOMER simulation tool. The optimization result showed that total 160 kW PV cell was required and the cost of electricity generation would be \$0.184. Additionally, the average solar radiation data of the location as well as the cost of the different component required for the setup was observed

Al-Messabi *et al.* (2016) reported that amongst non-conventional generators, photovoltaics (PVs) are becoming more popular owing to their relatively low costs and convenience. However, the intermittency of the PV generator outputs require accurate forecasting, planning, and optimal management. Existing forecasting methods, which are based on either clear-box or black-box modelling, have room for improvement, especially in the accuracy of capturing the underlying PV characteristics and forecasting of PV yields by explores the use of a priori knowledge of PV systems to models. Forecasting performance was improved and offers a new approach to practical system modelling but not simulated.

Okello *et al.* (2015) analyzed and compared the actual measured and simulated performance of a 3.2 kWp grid-connected photovoltaic system. The system was located at the Outdoor Research Facility (34.01°S, 25.67°E) at the Nelson Mandela Metropolitan University (NMMU), South Africa. The system consisted 14 poly crystalline silicon modules connected in two strings of 7 series-connected modules, each facing north at a fixed tilt of 34°. The data presented in this study were measured in the year 2013, where the system supplied a total of 5757 kWh to the local electric utility grid. The performance of the system was simulated using PVSYST software using measured and Meteonorm derived climate data sets (solar radiation, ambient temperature and wind speed). The comparison between measured and simulated energy yield were discussed. Both simulation results gave good approximation to measured energy output but better comparison between measured monthly energy outputs was obtained with simulation results performed using measured solar parameters. This implies that Meteonorm derived parameters can be used to estimate the performance of PV

systems within Eastern Cape region with a reasonable accuracy but the simulation accuracy can be improved by using on-site solar resource measurements.

Ramli *et al.* (2015) analyzed the optimal photovoltaic (PV) array and inverter sizes for a grid-connected PV system. Unmet load, excess electricity, fraction of renewable electricity, net present cost (NPC) and carbon dioxide (CO₂) emissions percentage were considered in order to obtain optimal sizing of the grid-connected PV system. An optimum result, with unmet load and excess electricity of 0%, for serving electricity in Makkah, Saudi Arabia was achieved with the PV inverter size ratio of $R = 1$ with minimized CO₂ emissions. However, they pointed out that inverter size can be downsized to 68% of the PV nominal power to reduce the inverter cost, and hence decrease the total NPC of the system.

2.4 Application of HOMER on Solar Photovoltaic

Many studies have been done addressing simulation, evaluation and performance analysis of solar Photovoltaic (Saidur *et al.*, 2012). However, most of them considered small and microscale solar energy using data and software (Nair and Garimella, 2010). Few studies consider a large scale and small-scale grid connected with different characteristics including I-V characteristics. The grid plays an important role of a backup power component in the system when the generating energy resource is enough to meet the load and the excess of the energy to be sold as feed-in-tariff (Couture and Gagnon, 2010).

Therefore, this research will perform a thorough simulation, performance analysis and improvements of the solar farm installed at KIST as well as NM-AIST and the economic analysis will be performing using HOMER software. The process modeling in HOMER will take into account the meteorological data, load curves, and cost of the components.

CHAPTER THREE

MATERIALS AND METHODS

3.1 Study Locations

In this study, the work was conducted in two locations (i.e KIST, Zanzibar and NM-AIST, Arusha). At KIST, experimental work and HOMER simulations were conducted. Experiments included investigation of the impact of distance from the roof to the panel, reflection and inclination angles. At NM-AIST only HOMER simulations were conducted using the data recorded from the data logger installed in order to investigate the performance of the system.

3.2 Instruments

The instrument used in this study were multimeter (model INNOVA 3300), for measuring short circuits currents and open circuit voltages. The short-circuit current (I_{sc}) is the current through the solar PV when the voltage across the solar cell is zero (i.e., when the solar PV is short circuited) and the open-circuit voltage, V_{oc} , is the maximum voltage available from a solar cell, and this occurs at zero current. The energy can be calculated from equations (1), (2) and (3).

3.3 Technical Data

Solar panels are rated to perform according to their specifications under standard test conditions (STCs) – a condition that can be created in a lab to allow easy measurement and comparison. The defined STCs for solar is when a panel is pointed directly at a bright sun with 1000 W of solar energy landing per square meter, with the panel kept at 25 degrees Celsius (77 degrees Fahrenheit) and an atmospheric mass (a number that refers to the amount of atmosphere between the panel and the sun) of 1.5 overhead. Table 1 illustrates technical details of the existing PV panels that were investigated in this study.

Table 1: Technical detail of the systems

Designation	KIST Administration	KIST dining hall	NM-AIST
Power	25.21 kW _p	50.42 kW _p	0.3kW _p
Area	176.94 m ²	353.88 m ²	4.07 m ²
Tracking system	Without tracking system	Without tracking system	Without tracking system
Tilt	30°	30°	30°
Orientation	0°	0°	0°
Type of installation	Roof top installation, small distance (<10 cm)		>10 cm
System start-up	31/10/2013		July 2017
Series-connected	15	15	2
Parallel-connected	2	2	2
Inverter type	SMA SMC 8000TL		WINKLE POWER
Number of inverters	3	6	1
Module type	Hanwha SF260 Poly (280W)		Si-3000S (150W)
Number of modules	90	180	4

3.4 Site location and Systems specific information

KIST is located at the latitude -6.16 (6°09'36"S), longitude +39.2 (39°12'00"E) and altitude 0 m at a distance of 72 km above the Indian Ocean while NM-AIST is located at the latitude -3.4 (3°24'0"S), longitude +36.78 (36°47'8"E) in Arusha region on north of Tanzania. Site-specific information and system description are shown in Table 2 below.

Table 2: Systems specific information

Description	Daily values		Unit
	KIST	NM-AIST	
Sum of global radiation	4.51	4.51	kWh/m ²
Energy	258.17	7.2	kWh
Specific energy	3.41	-	kWh/kW _p
Nominal output	75.63	0.3	kW _p

3.5 Current and Voltage Measurements (D.C Measurements)

The open-circuit voltage (V_{oc}) and the short-circuit current (I_{sc}) cannot be measured at the same time because they correspond to different operating modes of the device. During short-circuit current (I_{sc}) an ammeter was connected to solar PV for measuring current generated by the panel (Ellabban *et al.*, 2014). The voltage is created between the contacts because of the charge-separating element of a solar PV. For measuring the voltage, voltmeter was connected between two points of the module terminals (parallel connection). Figure 1 shows the arrangement of the PV modules and other more specifications for the solar modules in each site are shown in Table 3.



Figure 1: KIST PV System arrangement

Table 3: Specification of solar panel

Quantity	Symbol	Unit	KIST Values		NM-AIST Values	
			STC	NOCT	STC	NOCT
Maximum power rating	P_{max}	W	280	204	150	108
Open circuit voltage	V_{oc}	V	44.3	40.8	22.19	20.2
Sort-circuit current	I_{sc}	A	8.45	6.84	8.62	6.9
Rated voltage at max. power	V_{mpp}	V	36.2	32.9	18.16	16.2
Rated current at max. power	I_{mpp}	A	7.87	6.21	8.06	6.7
Module efficiency	H	%	14.3	14.3	14.88	14.88
Weight	W	Kg	11.6	11.6	12	12
Dimensions	-	mm	1483*668*35		1510*674*50	
Maximum system voltage	V_{max}	V_{DC}	1000	1000	1000	1000
Wind resistance	-	P_a	2400	2400	2400	2400

3.6 The Grid Connected PV System at KIST and NM-AIST

The grid connected PV system at KIST consists 180 modules tilted at a fixed angle of 30° and oriented northward covering a total area of 531 m^2 (admission and dining hall) as shown in Fig. 2. The system started to operation since October 2013. Grid connected data were recorded using power conditioning devices (Model: SMA SMC 8000TL) from 7:15 to 17:30 hours at intervals of 15 minutes. Monthly average data were therefore used for analyzing the performance (power and energy) of the solar farm.

The data (measurements) from NM-AIST grid connected PV system was obtained by reading from the module Si-3000S from the installed data logger as shown in Fig. 2 and 3.



Figure 2: Installed rooftop solar PV at KIST



Figure 3: Installed rooftop solar PV at NM-AIST

The block diagrams of the systems are as shown in Fig. 4 and 5 for KIST and NM-AIST respectively.

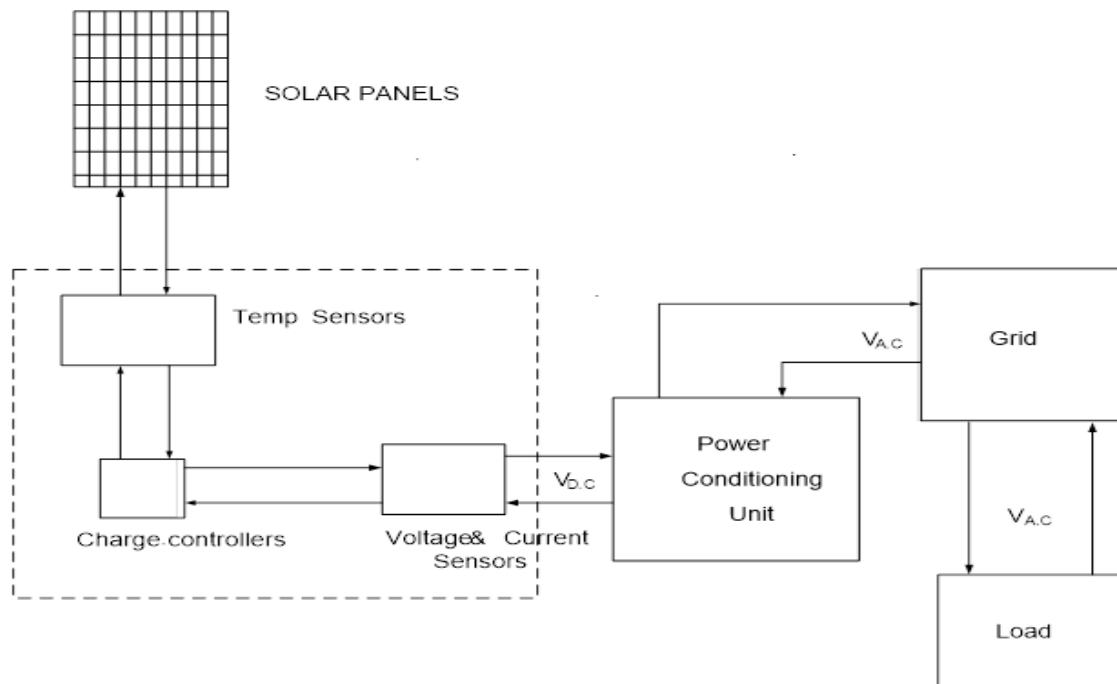


Figure 4: Block diagram of grid connected KIST-PV system

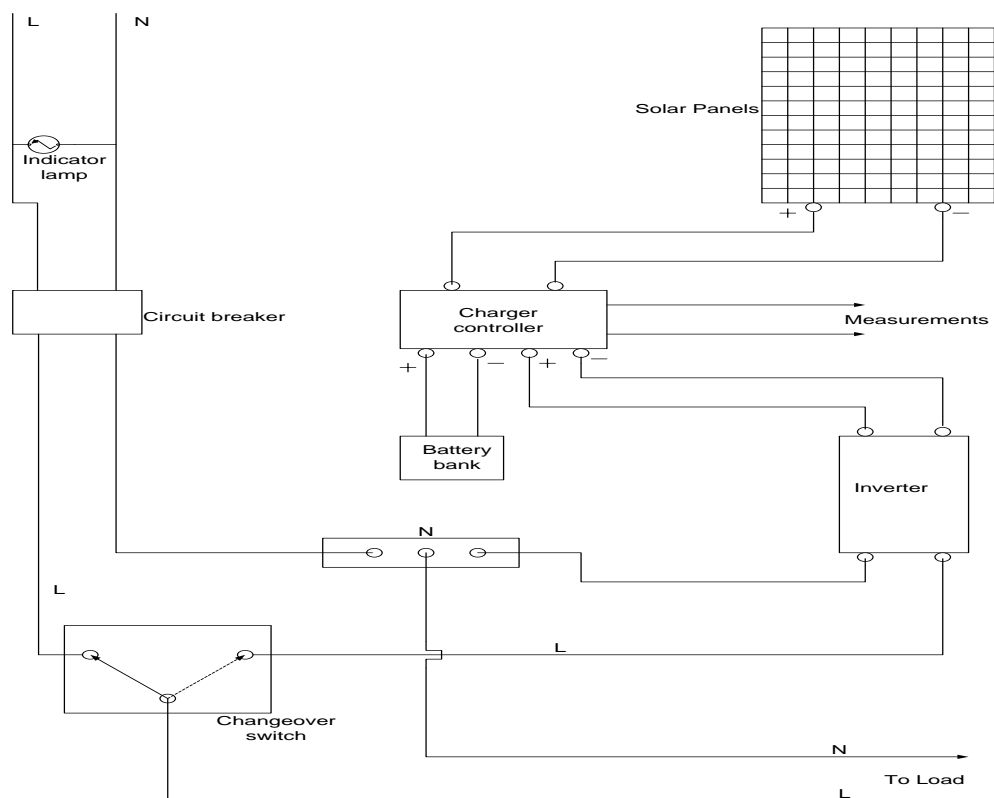


Figure 5: NM-AIST PV System arrangement

3.7 Performance Parameters

In a grid connected PV system the factors that represents the performance of the PV system include: energy/power output, reference yield, array yield, final yield, system energy losses, system efficiencies and inverter efficiency, performance ratio and capacity factor (Sharma and Goel, 2017) and were calculated using equations 1 – 13. The data collected from 2014, 2015 and 2016 were used for computing the listed parameters.

Energy output ($E_{A.C}$) is defined as the amount of alternating current (AC) power generated by the system over a given period of time. The total hourly, daily and monthly energy produced can be determined respectively as:

$$E_{A.C,h} = \sum_{t=1}^{60} E_{A.C, t} \quad (1)$$

$$E_{A.C,d} = \sum_{h=1}^{24} E_{A.C, h} \quad (2)$$

$$E_{A.C,m} = \sum_{d=1}^N E_{A.C, d} \quad (3)$$

where $E_{A.C,t}$ is AC energy output at time t (in min);

$E_{A.C,h}$ is AC energy output at hour h ;

$E_{A.C,d}$ is the daily AC energy output;

$E_{A.C,m}$ is the monthly AC energy output and

N is the number of days in a month.

Array yield (Y_a) is the ratio of power output from the PV (P_{dc}) to its rated power ($P_{pv \text{ rated}}$) and it is given by

$$Y_a = \frac{P_{dc}}{P_{pv \text{ rated}}} \times 100\% \quad (3)$$

Final yield (Y_{Fd} or Y_f) is the net energy output E_{PV} divided by the nameplate d.c power $P_{maxG,STC}$ (STC – Standard Test Condition 1000 W/m^2 , 25° C) of the installed PV array. It represents the number of hours that the PV array would need to operate at its rated power to provide the same energy. The units are hours or kWh/kW. It is defined as the ratio of net daily/month/annual A.C power output of the system which was supplied ($P_{A.C}$) to the rated power of the installed PV.

$$Y_{Fd} = \frac{P_{A.C}}{P_{pv \text{ rated}}} \times 100\% \quad (4)$$

Reference yield (Y_r) is the total in-plane irradiance H divided by the PV's reference irradiance G . It represents the under ideal conditions obtainable energy. If G equals 1 kW/m^2 , then Y_r is the number of peak sun hours or the solar radiation in units of kWh/m^2 . The Y_r

defines the solar radiation resource for the PV system. It is a function of the location, orientation of the PV array, and month-to-month and year-to-year weather variability. It is the total daily solar irradiance (G_a kWh/m²) divided by reference irradiation ($G_i = 1$ kW/m²). This represents the number of hours for peak sun per day (h/d).

$$Y_r = \frac{G_a}{G_{i\ ref}} = \frac{G_a}{1kW/m^2} \quad (5)$$

PV module efficiency (η) is given by

$$\eta(PV) = \frac{V_{mpp} \times I_{mpp}}{Area \times Average\ irradiance} \quad (6)$$

where the V_{mpp} and I_{mpp} are maximum power points for voltage and current, respectively

The I-V characteristic is shown in Figure 6.

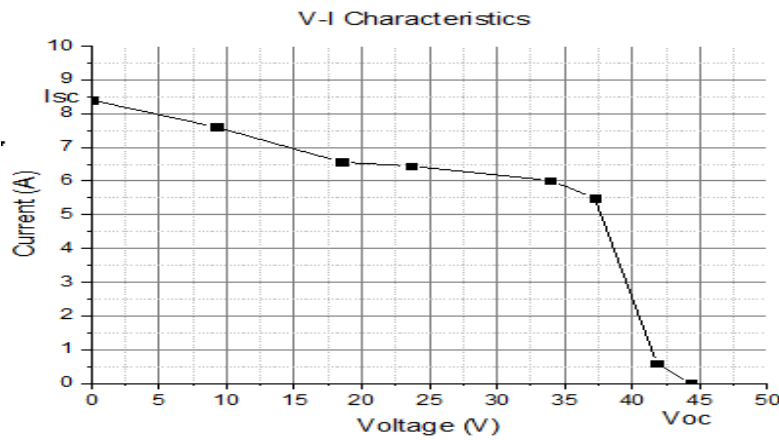


Figure 6: I-V Characteristics

From the Fig. 5 above the V_{mpp} and I_{mpp} are 37.5V and 6.01A respectively

If the cell temperature (T) has been changed then

$$\eta_{pv} = \eta_{ref} [1 - \beta_{ref}(T - T_{ref})] \times 100\% \quad (7)$$

where β_{ref} is the temperature coefficient

η_{ref} is reference efficiency of PV module at reference temperature

T_{ref} is reference temperature

Hence the nominal operating cell temperature of module declared by manufacture (NOCT) is reached in nominal incident condition under an irradiance of 800 W/m² at ambient temperature ($T_{ambient}$) and room temperature is taken as 25°C. Then,

$$T = T_{ambient} + \left(\frac{NOCT - 25}{800} \right) G_a \quad (8)$$

Inverter efficiency (η_{inv}) may vary from something just over 50% when a trickle of power is being used, to something over 90% when the output is approaching the inverters rated output and the inverter efficiency is given by

$$\eta_{inv} = \frac{P_{A.C}}{P_{d.c}} \times 100\% \quad (9)$$

Since solar cell efficiency refers to the portion of energy in the form of sunlight that can be converted via photovoltaics into electricity. The efficiency of the solar cells used in a photovoltaic system, in combination with latitude and climate, determines the annual energy output of the system. The system efficiency (η_{sys}) can be calculated as

$$\eta_{sys} = \frac{P_{A.C}}{G_a \times \text{Area of the PV}} \times 100\% \quad (10)$$

where $P_{A.C}$ is the A.C power

$P_{d.c}$ is the d.c power

G_a is the solar insolation in kW/m²/day

The performance ratio (PR) is defined in IEC 61724 and is a metric commonly used to measure solar photovoltaic (PV) plant performance for acceptance and operations testing. The PR measures how effectively the plant converts sunlight collected by the PV panels into AC energy delivered to the off-taker relative to what would be expected from the panel nameplate rating. This metric quantifies the overall effect of losses due to: inverter inefficiency, wiring, cell mismatch, and elevated PV module temperature, reflection from the module front surface, soiling, system down-time, shading, and component failures. Because many of these factors are indicators of build quality, this metric is popular with some companies and financiers for contractual acceptance testing. However, some of these factors are also weather dependent. Most notably, weather affects the PR by affecting the module temperature.

It indicates the overall offset of losses for the rated power output due to PV temperature of the module, inverter efficiency and other factors. Performance ratio is the ratio of power fed to the grid (final yield) to the power that the system could have produced at dc rated power for the number of peak sun hours per day (Marion *et al.*, 2005).

$$P.R = \frac{E_{A.C}}{P_{D.C} \times \text{Operating hours}} \quad (11)$$

The Capacity factor (C.F) of a renewable generator is calculated by one of several methods. Detailed reliability-based metrics are widely accepted by utilities and system planners. These

methods use statistical approaches to determine the ability of a generation resource to maintain a reliable system and meet demand. An alternative approach is to use approximation techniques, such as examining the output of a renewable generator during periods of highest risk of not meeting load. These are typically hours of high demand, often late afternoons in summer, when the demand for air-conditioning places utility systems under greatest stress. Examining solar output during these periods can provide insight into the potential of different solar generators to add reliable capacity. The capacity factor or utilization factor is the ratio of annually energy generated by the PV ($E_{A.C}$) to the amount of energy that the PV would generate at the operation hours.

$$C.F = \frac{E_{A.C}}{P_{PV-rated} \times 24 \text{ hours} \times 365} \times 100\% \quad (12)$$

The total Energy loss (L_T) is given by

$$L_T = Y_r - Y_{Fd} \quad (13)$$

3.8 Simulation using HOMER Software

HOMER software developed by the National Renewable Energy Laboratory, Department of Energy in the United States was used for optimization of renewable energies at KIST and NM-AIST. This software allows the user to input an hourly power consumption profile and match renewable energy generation to the required load. It allows a user to analyze micro-grid potential, peak renewables penetration, ratio of renewable sources to total energy, and grid stability, particularly for medium to large scale projects. Additionally, HOMER contains a powerful optimizing function that is useful in determining the cost of various energy project scenarios. HOMER functionality allows minimization of leveled cost of energy. The systems configurations are as shown on Fig. 7.

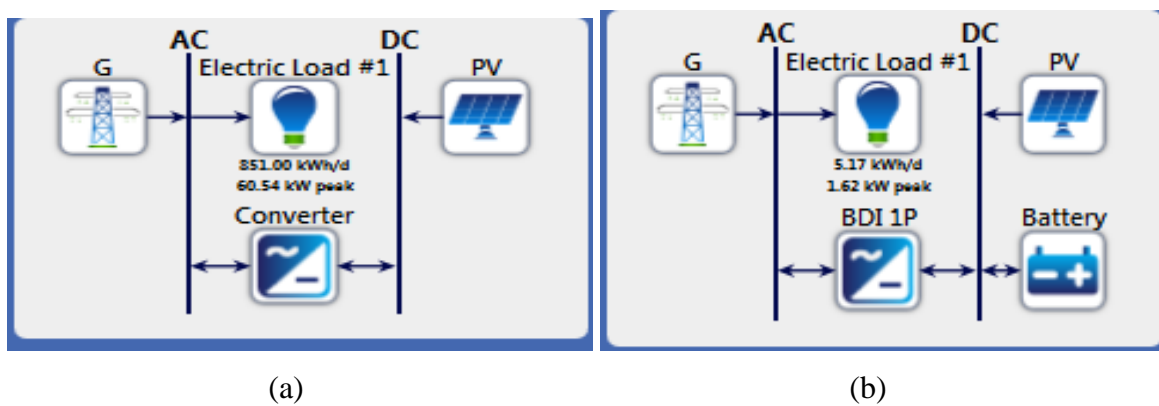


Figure 7: Systems configuration (a) KIST and (b) NM-AIST

This study is divided into two sections; the first section shows how HOMER can be used to optimize renewable energy system based on the net present cost of the system from a list of different possible configuration. The second section reports the investigation of the effects of different load profiles.

The inputs provided are technology options, component costs and resource availability. HOMER software uses these inputs to simulate different system configurations, or combinations of components, and grid results that can be viewed as a list of feasible configurations sorted by net present cost. Tables 5 – 8 and Fig. 7 - 9 shows all input data for the two systems at KIST and NM-AIST.

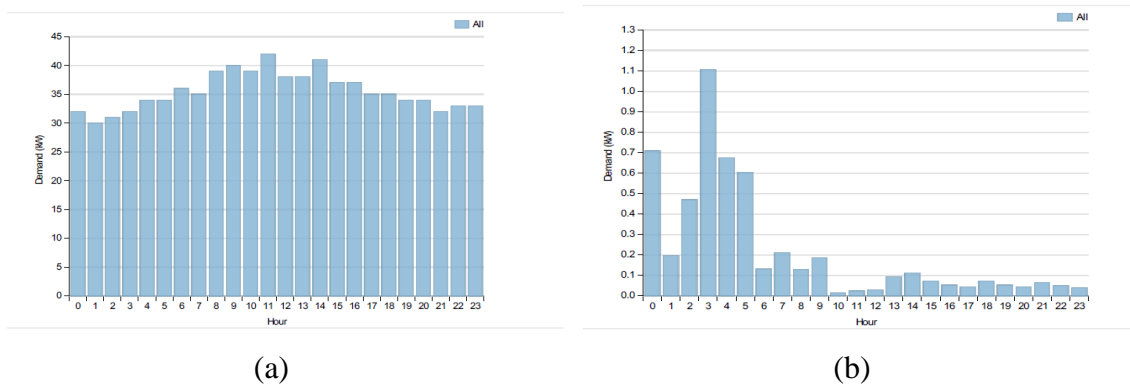
HOMER performs the energy balance calculations, system cost calculations for each of the considered system configuration as shown in Fig. 6(a) and 6(b) listing all of the possible system sizes, sorted by Net Present Cost (NPC). Additionally, the software includes several energy components and evaluates suitable options considering cost and availability of energy inputs like component type, capital, replacement, operation and maintenance costs, efficiency, operational life, etc. are also required for both grid-connected and stand-alone systems have been investigated, consisting of installed PV energy sources and conventional systems.

The demonstration-level and experimental PV systems energy sources have much focused on the installation of the PV energy sources without enough and thorough investigation of the feasibility and the optimal combination of the resources and thus have met numerous problems including failure to meet the load demand, economically unacceptable system configuration. Table 4 shows all input summary of the systems.

Table 4: Systems input data

	QUANTITY	KIST	NM-AIST
LOCATION	Location	(UR) Zanzibar Town, Tanzania	Nyerere Rd, Tanzania
	Latitude	6 degrees 12.96 minutes South	3 degrees 23.99 minutes South
	Longitude	39 degrees 12.45 minutes East	36 degrees 47.81 minutes East
	Time Zone	Africa/Dar es Salaam	Africa/Dar es Salaam
LOAD	Data source	Synthetic	Synthetic
	Daily noise	10%	10%
	Hourly noise	10%	10%
	Scaled annual average	851.000 kWh/d	5.167 kWh/d
	Scaled peak load	60.5395 kW	1.6159 kW
	Load factor	0.5857	0.1332

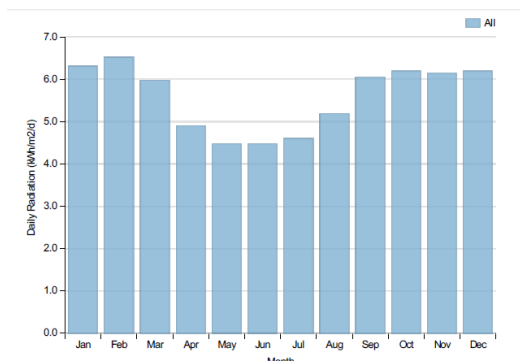
The load curves for KIST shows that at all hours the load is there but in NM-AIST the pick load seemed at night hours because only at these hours the system is in operation.

**Figure 8:** Systems load curve (a) KIST and (b) NM-AIST**Table 5:** Systems cost input for Generic flat plate PV

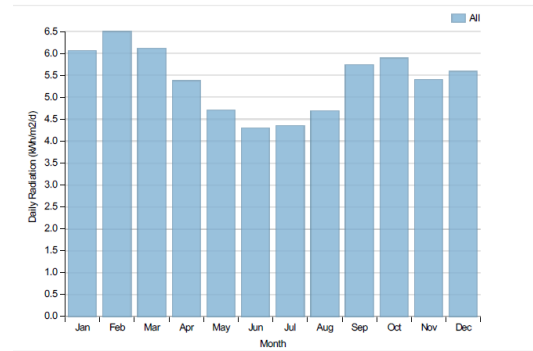
Site	Size (kW)	Capital	Replacement	O&M
KIST	0.28	\$1100.00	\$660.00	\$10.00
NM-AIST	0.15	\$600.00	\$400.00	\$10.00

Table 6: System configuration inputs

Quantity	KIST	NM-AIST
Sizes to consider (kW)	30, 40, 50, 70, 80	0.3, 0.4, 0.5, 0.6, 1
Lifetime	25 years	25 years
Derating factor	80%	80%
Tracking system	No Tracking	No Tracking
Slope	6.216 deg	3.400 deg
Azimuth	180.000 deg	180.000 deg
Ground reflectance	20.0%	20.0%
Scaled annual solar insolation	5.58 kWh/m ² /d	5.39 kWh/m ² /d



(a) KIST



(b) NM-AIST

Figure 9: Systems solar insolation**Table 7:** Systems converter costs and inputs

Site	Size (kW)	Capital	Replacement	O&M
KIST	100	\$3000.00	\$1800.00	\$10.00
NM-AIST	1	\$600.00	\$600.00	\$10.00
Quantity	KIST		NM-AIST	
Sizes to consider in kW	25.21, 40, 50.42, 75.63, 100		5, 4, 3	
Lifetime	10 years		10 years	
Inverter can parallel with AC generator	Yes		Yes	

Battery: Generic 1kWh Lead Acid**Table 8:** Systems battery costs and specification

Site	Size (kW)	Capital	Replacement	O&M
NM-AIST	4	\$300.00	\$300.00	\$10.00
Quantities to consider			0, 1	
Voltage for each battery			12V	
Nominal capacity			83 Ah	
Lifetime throughput			800 kWh	

CHAPTER FOUR

RESULTS AND DISCUSSION

4.1 Performance Investigation at KIST

The performance of the systems was investigated in terms of impact of distance from the roof to the panel, impact of reflector using aluminum foil and the influence of angle of inclination. For each experiment I_{sc} and V_{oc} were measured and used to compute power output as described in the sections to follow:

4.1.1 Impact of Distance from the Roof

The results for the impact the of distance from the roof shows that the higher distance of 20 cm was improved by an increment of 1.85% compared to the existing distance of <10 cm because of high sensitivity and weather condition as shown in Fig. 10 and Appendices 1.

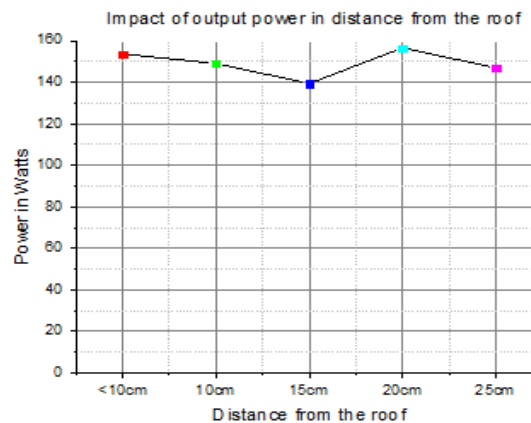


Figure 10: Impact of distance from the roof to output power

4.1.2 Impact of Reflector

The results of the impact of reflectors (aluminum foil was used) are shown in Fig. 11 and Appendix 1. It was seen that at 45° the power outputs were higher than other tested angles. This was because the loss of light was reduced as reflectors were used as light concentrators to the PV panels. The power output was increased by 1.3%.

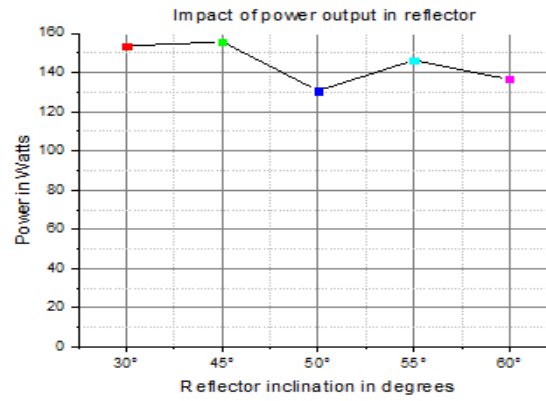


Figure 11: Impact of different inclination for the reflector to output power

4.1.3 Impact of Angle of Inclination

In inclination (angle of erecting the solar PV), the angle of 20° had better performance with an increment of 1.74% compared to the other angle of inclination as depicted in Fig. 12 and Appendix 1. This was because solar intensity to the PV panel was improved due to the decreased angle of incidence however during the experimental the wheather was varied. In addition, good inclination angle may reduce the accumulation of dust on PV panel hence reduce losses.

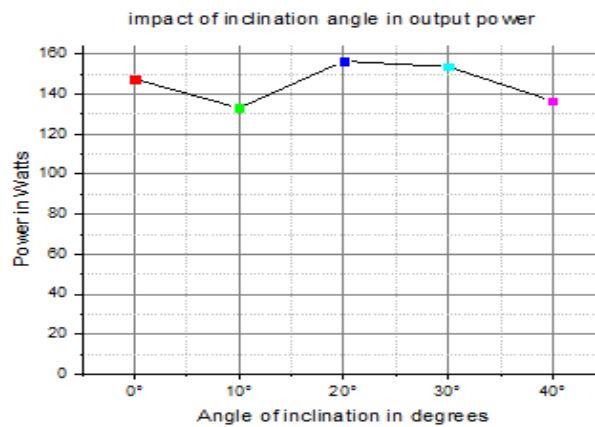


Figure 12: Impact of angle of inclination to output power

4.2 Grid-Tied Parameters Analysis at KIST

The measurements on parameters carried out that shows the same parameters measured of injected power and power demanded by the load may influence changes on the system (as recorded from the data logger). Some measured values are compared with the limits set in the international standards and hence are analyzed for three years (i.e 2016, 2015 and 2014).

It was observed that the minimum average solar insolation was in May and June (4.47 kWh/m²/day) and the maximum was in February (6.52 kWh/m²/day). The average array, final and reference yields were 0.063, 0.053 and 0.006 kWh/kW_p/day respectively. The highest final yield of 0.006 kWh/kW_p/day was recorded in January, February, July, August, November and December.

4.2.1 Direct Current Energy Produced and Alternating Current Energy Injected to Grid

It was observed that both D.C energy produced and A.C energy injected to grid are high at the year 2015 because of high production of energy as shown in Fig. 13.

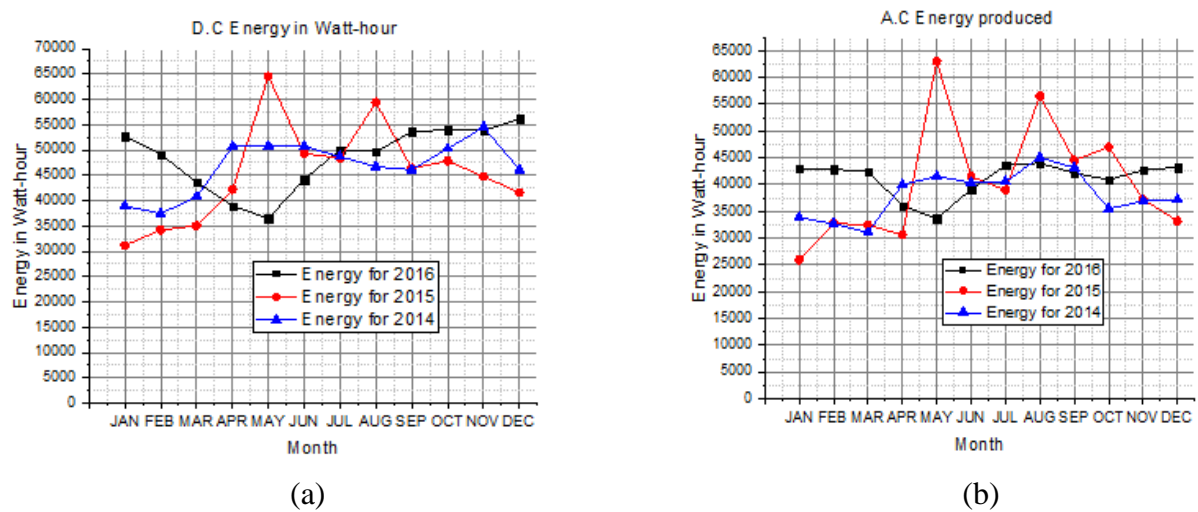
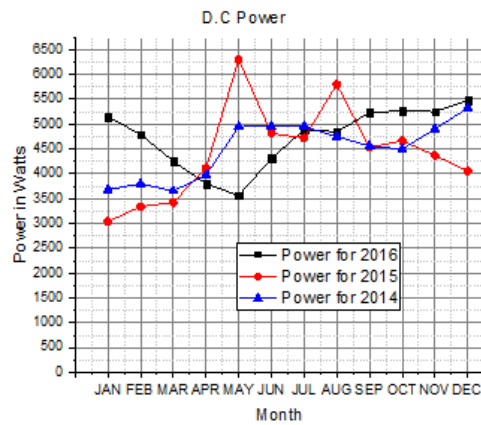


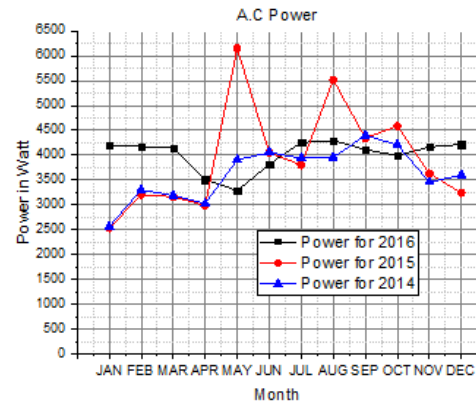
Figure 13: Energy in Watt-hour (a) D.C Energy produced (b) A.C Energy injected

4.2.2 Power Input to Inverter and Power Output from Inverter

It was observed that both power input to inverter and power output from inverter are high at the year 2015 because of high production of energy as shown in Fig. 14.



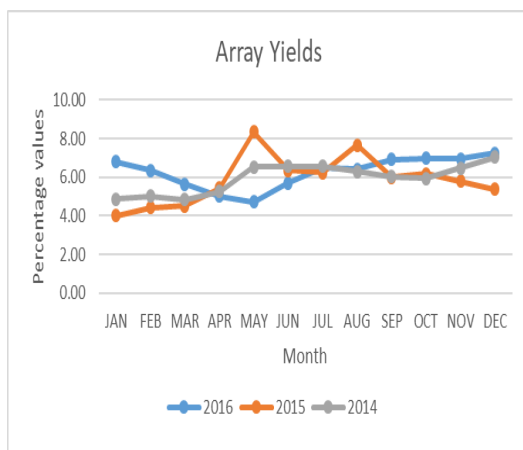
(a)



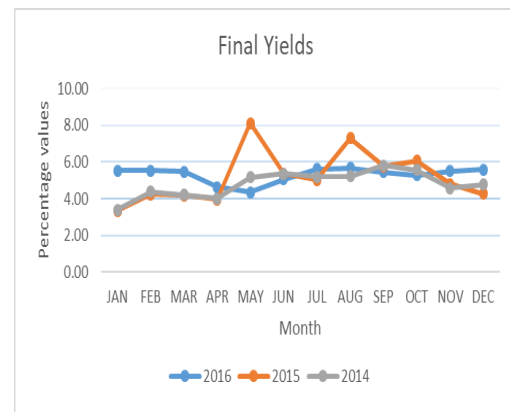
(b)

Figure 14: Power in Watts (a) Input to inverter (b) Output from inverter

It was observed that both array yield, temperature, final yield ratio, inverter efficiency, system efficiency, performance ratio, capacity factors are high at the month of May 2015 because of high production of energy as shown in Fig. 15, 16, 17(b) and 18, respectively. The average for inverter and system efficiencies was analyzed 85.46% and 11.15%, respectively. Additionally on load PV efficiency was better at 2016 because at December 2015 becomes zero since the system was off as shown in Fig. 17 (a). The temperature remain constant for the year of 2014, 2015 and 2016 months.

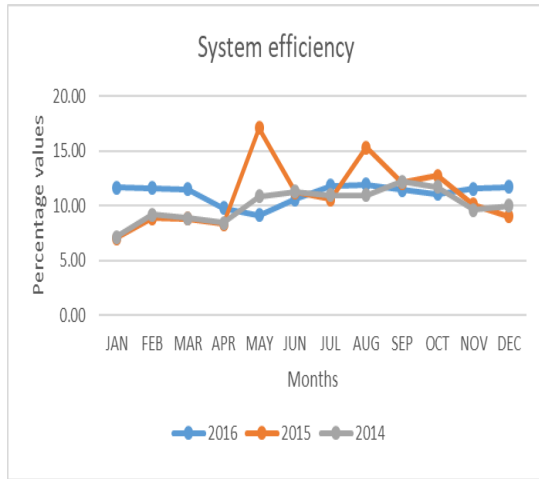


(a)

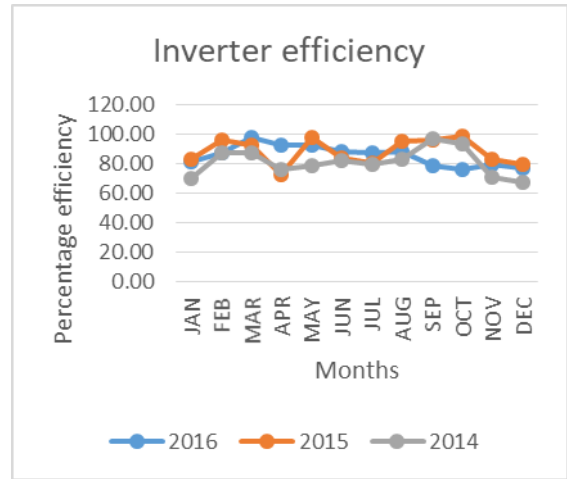


(b)

Figure 15: Yield ratios (a) Array yield (b) Final yield

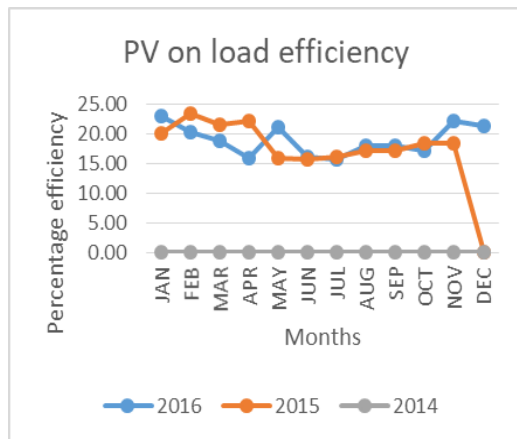


(a)

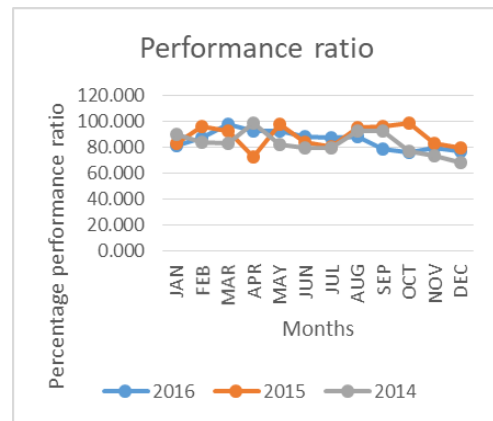


(b)

Figure 16: Efficiencies (a) System (b) Inverter

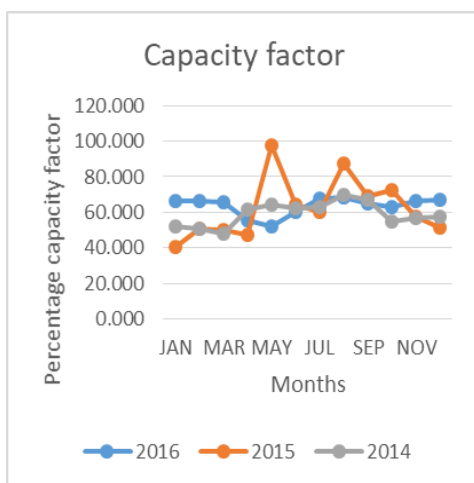


(a)

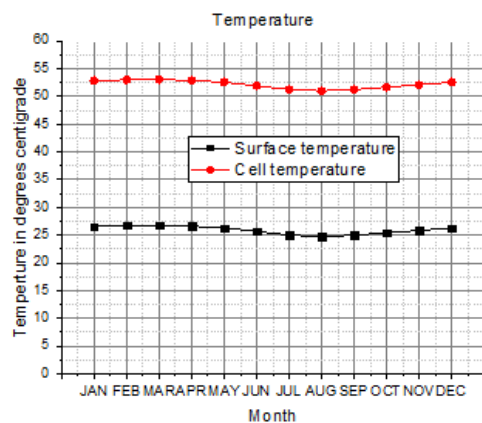


(b)

Figure 17: PV observation (a) On load efficiency (b) Performance ratio



(a)



(b)

Figure 18: Factors for the PV module (a) Capacity factor (b) Temperature

4.2.3 Grid connected results at KIST

In grid connected system, the value of current and voltage was used to obtain the power and energy values for both D.C and A.C values as shown in Appendix 2. In case of calculating the value of energy the power was multiplied by time of operation in hours.

4.3 Grid Connected PV System at NM-AIST

The results observed for the batteries at NM-AIST in a day. The battery has high voltages at 14:05 hours since charging capacity is high due to charged by charge controller. There are four batteries connected two series – parallel and gives the voltage to be 24 V. During charging of the battery, the voltage may rise $\pm 5\%$ for safe. Other voltages and time are as shown in Fig. 19.

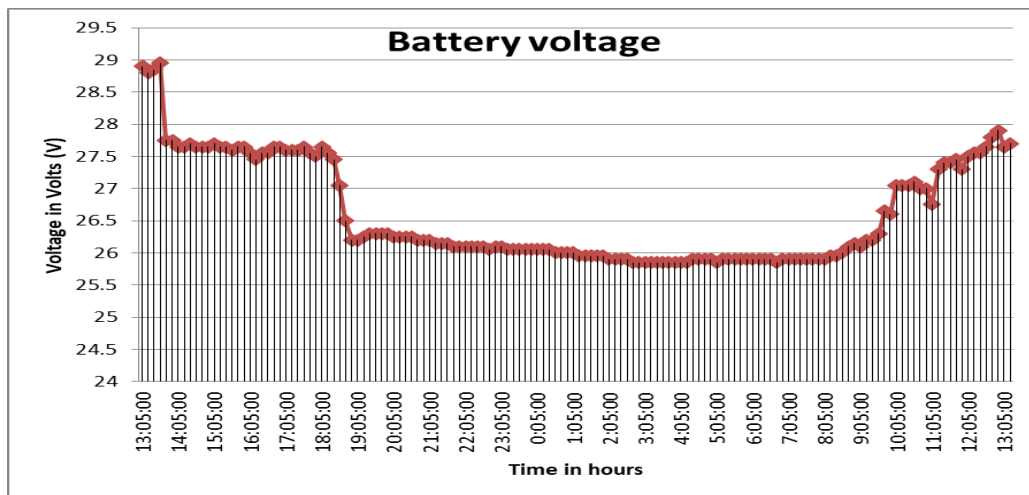
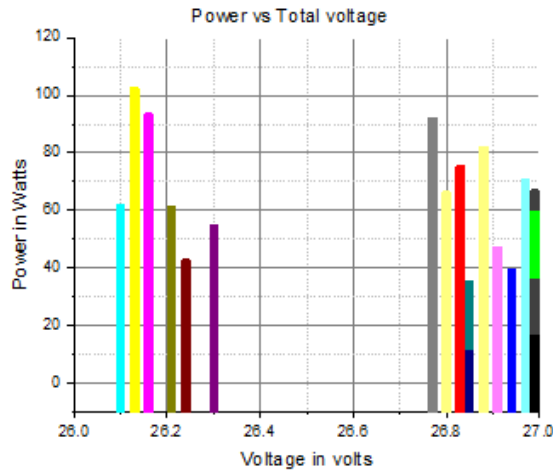


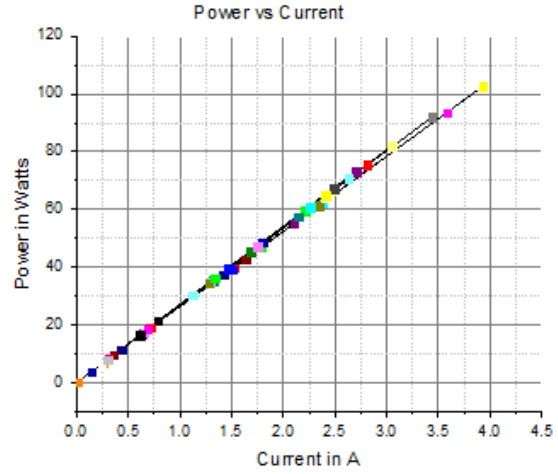
Figure 19: Battery voltages

4.3.1 Power vs Total voltage and Power vs Current

The results show that the power was high when the total voltage (the average voltage for north facing and south facing) is nearly 26.1V hence the operation is at maximum and the power was maximum and it was zero when disconnected from the system. The power vs voltage and power vs current characteristics for the system shown in Fig. 20.



(a)

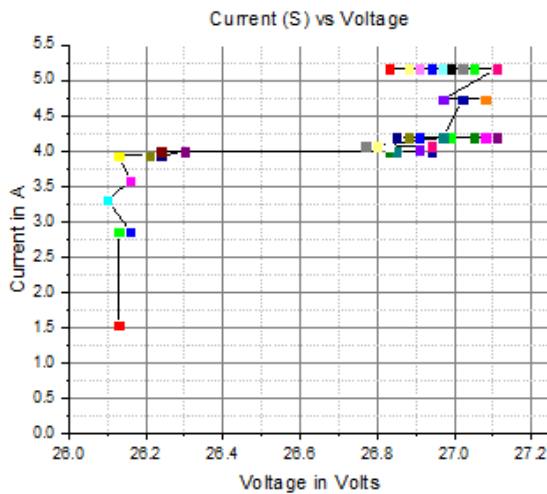


(b)

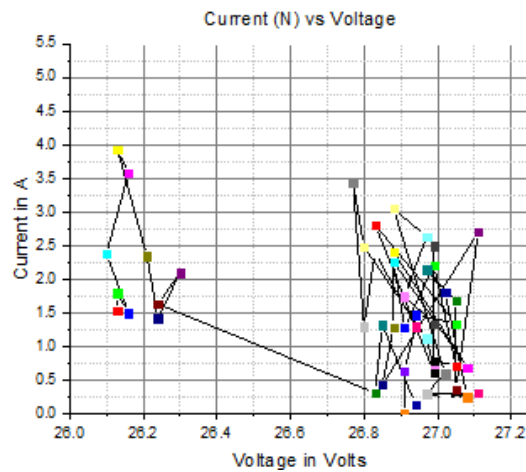
Figure 20: Power characteristics (a) Power vs total voltage (b) Power vs current

4.3.2 South facing Panels Current vs Voltage and North facing Current vs Voltage

The results shows that the value of voltages are not constants for both south facing currents and north facing current so that the graph are variegate, the ribbons and circles are the points where the value existing as shown in Fig. 21.



(a)



(b)

Figure 21: Panel facing current vs voltage (a) South facing panel current (b) North facing panel current

4.3.3 North facing Panels Voltage vs Currents and South facing Panels Voltage vs Currents

The results shows that the value of currents are constants for both north facing voltages and south facing voltages as shown in Fig. 22. Hence at any increase in voltage the current is in saturation (i.e fully charged).

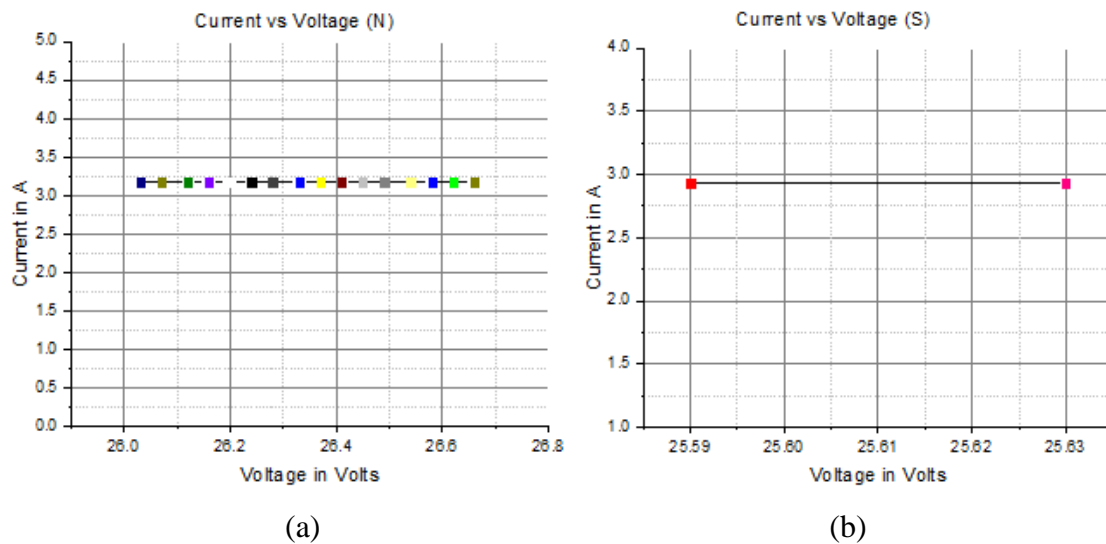


Figure 22: Current vs panel voltage (a) Current vs north facing panel voltage (b) current vs south voltage

4.4 HOMER Simulation

In simulation, HOMER determines technical feasibility and lifecycle costs of the systems for each hour of the year. In addition, the system configuration and the operation strategy of the supply components are tested to examine how these components work in a given setting over a period of time. After the simulation the results are shown in Fig. 32 - 40 and 41 -52 for KIST and NM-AIST respectively.

4.4.1 KIST Simulation Results

The simulation results observed that at 30 kW PV and 25.2 kW converter. The cost of energy (COE), net present cost (NPC), operating cost, initial cost and renewable fraction were \$0.118 /kWh, \$474 745, \$27 548, \$118 613 and 15% respectively. Other results for different outputs are as shown in Fig. 23.

Sensitivity cases: Overall													
Architecture				Cost				System	PV		Converter		G
PV (kW)	G	Converter (kW)	Dispatch	COE (\$)	NPC (\$)	Operating Cost (\$)	Initial Capital (\$)	Ren Frac (%)	Capital Cost (\$)	Production	Rectifier Mean Output	Inverter Mean Output	Energy Produced
30	999,999	25.2	CC	\$0.118	\$474,745	\$27,548	\$118,613	15	\$117,857	51,108	0	5	264,624
Optimization case: Overall													
Architecture				Cost				System	PV		Converter		G
PV (kW)	G	Converter (kW)	Dispatch	COE (\$)	NPC (\$)	Operating Cost (\$)	Initial Capital (\$)	Ren Frac (%)	Capital Cost (\$)	Production	Rectifier Mean Output	Inverter Mean Output	Energy Produced
30	999,999	25.2	CC	\$0.118	\$474,745	\$27,548	\$118,613	15	\$117,857	51,108	0	5	264,624
30	999,999	40.0	CC	\$0.118	\$475,294	\$27,556	\$119,057	15	\$117,857	51,108	0	5	254,520
30	999,999	50.4	CC	\$0.118	\$475,665	\$27,563	\$119,370	15	\$117,857	51,108	0	5	254,520
30	999,999	75.6	CC	\$0.119	\$476,630	\$27,577	\$120,126	15	\$117,857	51,108	0	5	254,520
30	999,999	100.0	CC	\$0.119	\$477,544	\$27,581	\$120,857	15	\$117,857	51,108	0	5	254,520
40	999,999	40.0	CC	\$0.124	\$499,401	\$26,382	\$158,343	20	\$157,143	68,114	0	7	249,348
40	999,999	50.4	CC	\$0.124	\$499,792	\$26,384	\$158,633	20	\$157,143	68,114	0	7	249,348
40	999,999	75.6	CC	\$0.125	\$500,737	\$26,401	\$159,412	20	\$157,143	68,114	0	7	249,348
40	999,999	25.2	CC	\$0.125	\$501,625	\$26,589	\$157,899	19	\$157,143	68,114	0	7	252,450
40	999,999	100.0	CC	\$0.125	\$501,651	\$26,417	\$160,143	20	\$157,143	68,114	0	7	249,348
50	999,999	40.0	CC	\$0.130	\$523,827	\$25,233	\$197,629	25	\$196,429	85,100	0	9	254,696
50	999,999	75.6	CC	\$0.130	\$525,096	\$25,248	\$198,697	25	\$196,429	85,100	0	9	234,666
50	999,999	100.0	CC	\$0.133	\$526,010	\$25,263	\$199,429	25	\$196,429	85,100	0	9	242,830
50	999,999	25.2	CC	\$0.133	\$534,365	\$26,062	\$197,185	22	\$196,429	85,100	0	8	211,992
70	999,999	50.4	CC	\$0.140	\$576,503	\$21,206	\$276,513	33	\$275,000	119,252	0	12	211,972
70	999,999	75.6	CC	\$0.140	\$576,660	\$21,159	\$277,269	34	\$275,000	119,252	0	12	211,972
70	999,999	100.0	CC	\$0.140	\$577,574	\$21,173	\$278,000	34	\$275,000	119,252	0	12	213,443
70	999,999	40.0	CC	\$0.144	\$582,113	\$21,664	\$276,200	32	\$275,000	119,252	0	11	204,262
80	999,999	75.6	CC	\$0.143	\$503,994	\$22,235	\$316,555	38	\$314,286	136,288	0	14	204,262
80	999,999	100.0	CC	\$0.141	\$504,908	\$22,249	\$317,246	34	\$314,286	136,288	0	14	204,321
80	999,999	50.4	CC	\$0.145	\$506,828	\$22,512	\$315,796	37	\$314,286	136,288	0	14	252,381
70	999,999	25.2	CC	\$0.152	\$508,532	\$25,742	\$275,736	25	\$275,000	119,252	0	9	252,383
80	999,999	40.0	CC	\$0.152	\$516,309	\$21,270	\$315,436	34	\$314,286	136,288	0	12	206,568
80	999,999	100.0	CC	\$0.143	\$504,908	\$22,249	\$317,266	38	\$314,286	119,252	0	14	204,262
80	999,999	50.4	CC	\$0.143	\$506,828	\$22,512	\$315,794	37	\$314,286	136,288	0	14	204,321
70	999,999	25.2	CC	\$0.152	\$508,532	\$25,742	\$276,756	25	\$275,000	119,252	0	9	232,283
80	999,999	40.0	CC	\$0.152	\$516,309	\$21,270	\$315,446	34	\$314,286	136,288	0	12	206,509
80	999,999	25.2	CC	\$0.162	\$548,068	\$25,761	\$315,042	28	\$314,286	136,288	0	9	208,966

Figure 23: Simulation results for KIST

4.4.2 Cash Summary (Annualized and Net Present)

The annually and net present cash summary by component results shows that the grid has higher costs about \$26 171 compared to PV modules in which costs \$22 983 for energy production as shown in Fig. 24 and 25, respectively.

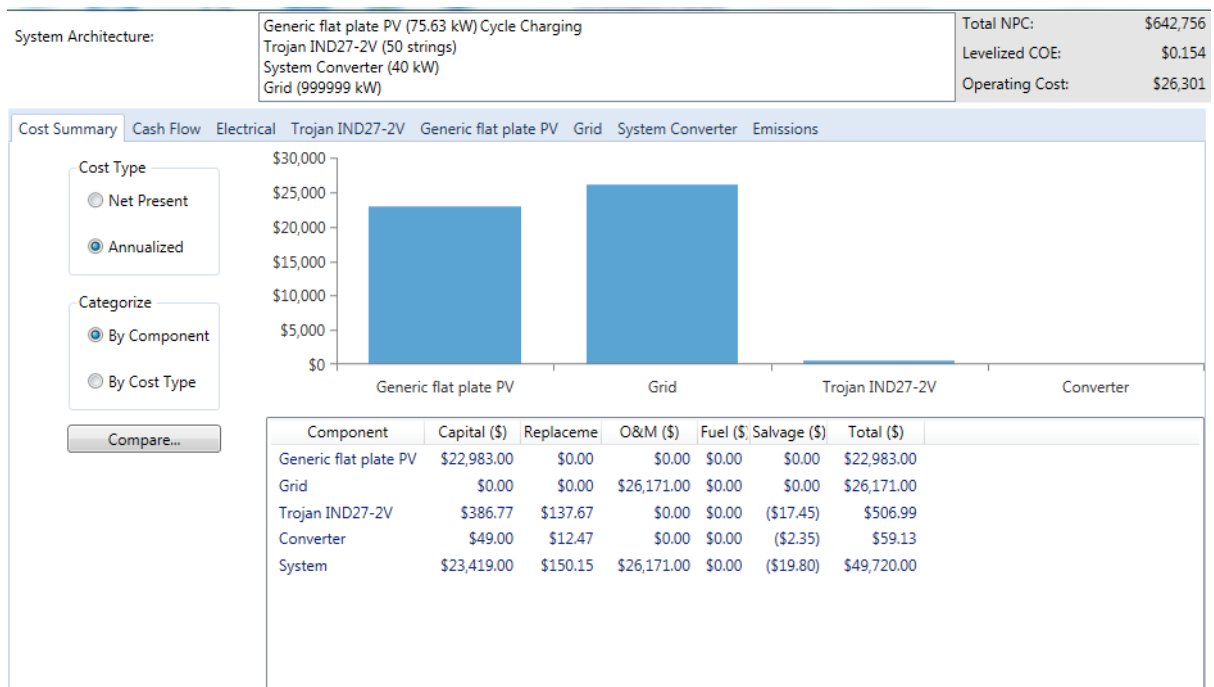


Figure 24: Cash summary (Annually by component) results for KIST

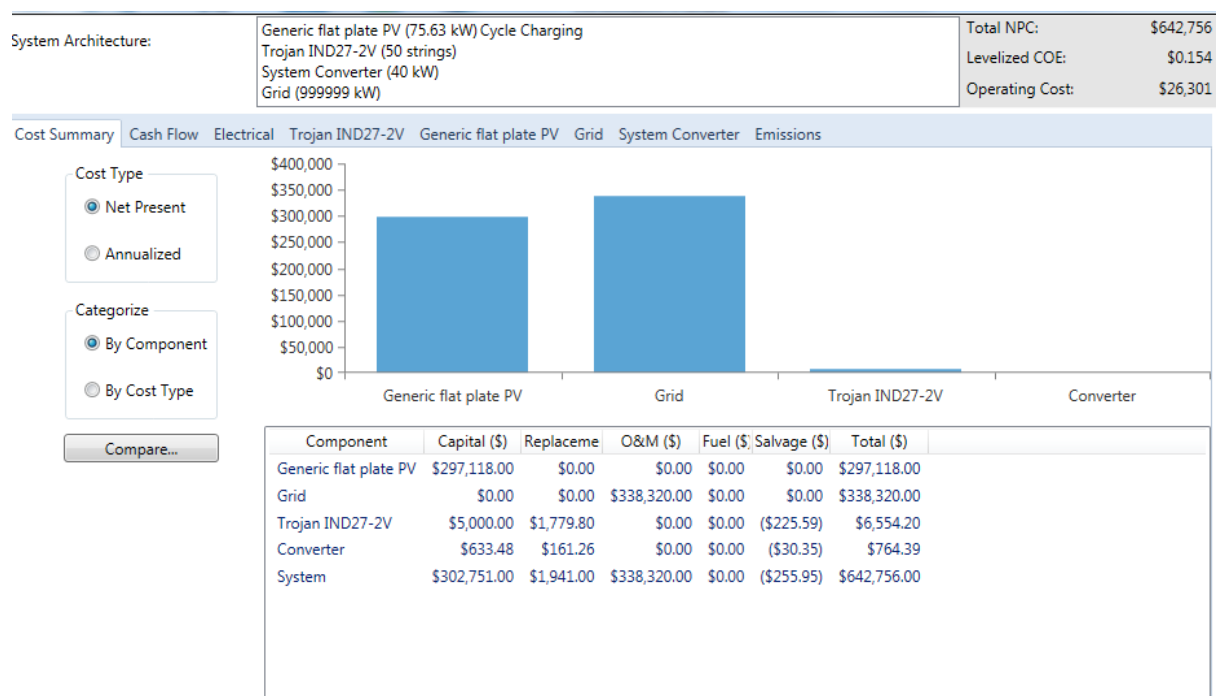


Figure 25: Cash summary (Net Present by component) results for KIST

4.4.3 Cash Summary (Annualized and Net Present) at KIST

The annually and net present cash summary by cost type results shows that the grid has higher costs about \$338 320 compared to PV modules which has the cost about \$297 118 for energy production as shown in Fig. 26 and 27, respectively.

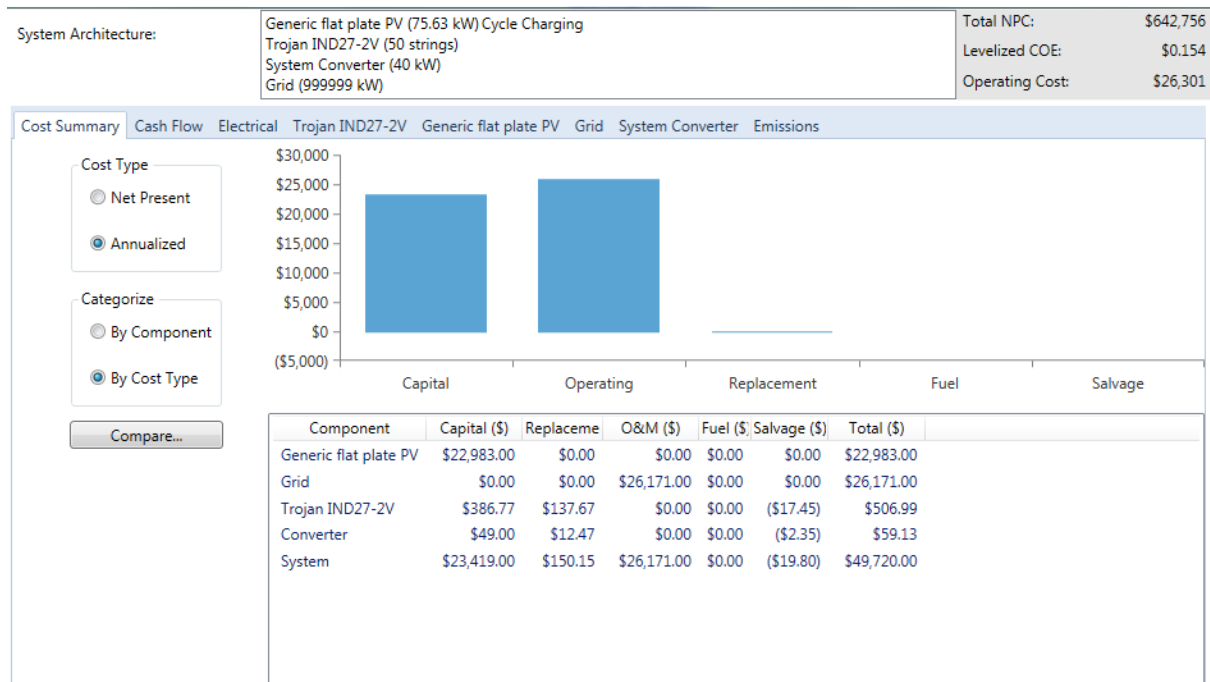


Figure 26: Cash summary (Annualized by cost type) results for KIST

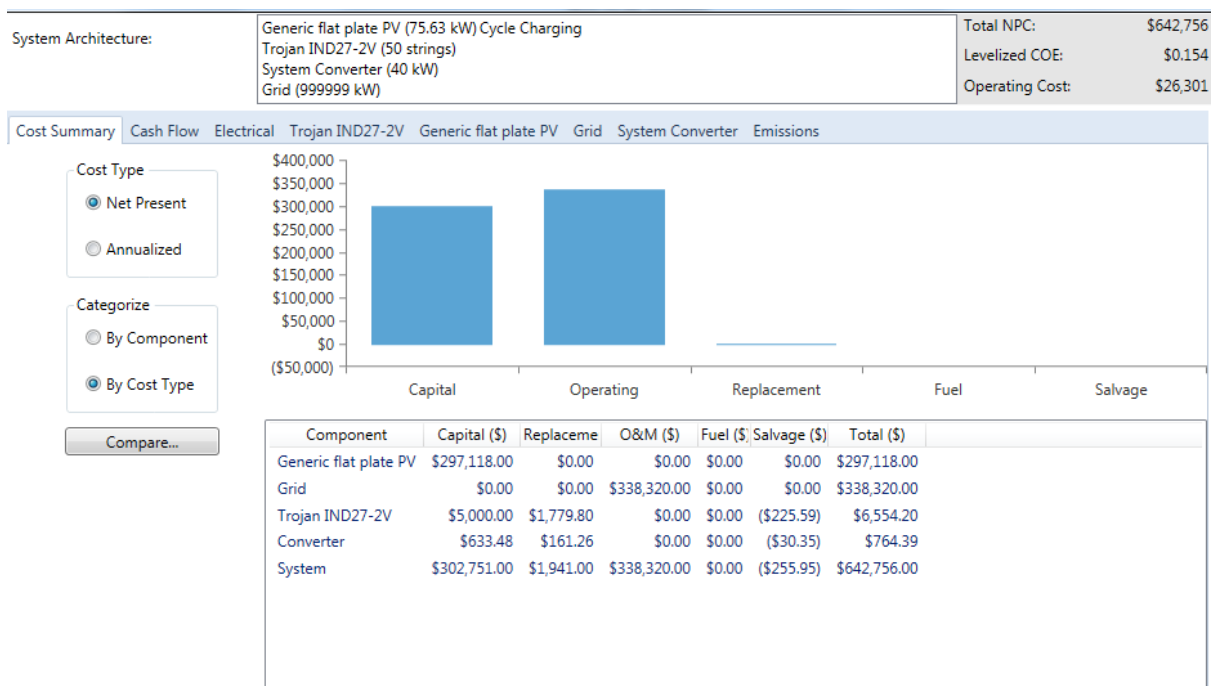


Figure 27: Cash summary (Net Present by cost type) results for KIST

4.4.4 Profile Time Series

The profile time series shows that the months of January, March, June, July, November and December have high and variable primary loads as shown in Fig. 28.

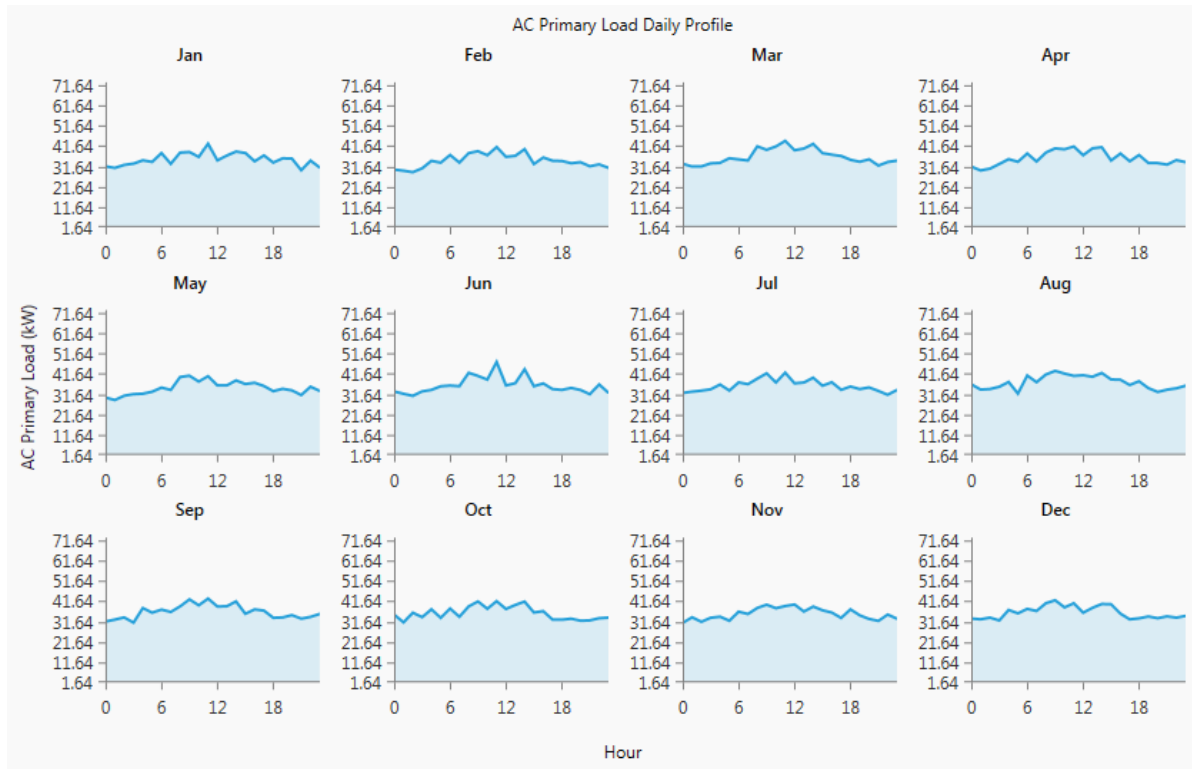


Figure 28: Profile time series results for KIST

4.4.5 Electrical Simulation

The electrical simulation shows that the PV modules production was 122 410 kWh/year and Grid purchase was 267 216 kWh/year equivalent to 68.58% and 31.42% of the total production respectively, the consumption rate for AC primary load was 33 866 kWh/year and grid sells was 8225 kWh/year equivalent to 97.4% and 2.6% of the total consumption respectively, the quality for excess of electricity: 55 955 kWh/year equivalent to 14.4% of the total quality. Additionally, the quality value for renewable fraction was 17 with maximum renewable penetration of 235.3 as shown in Fig. 29.

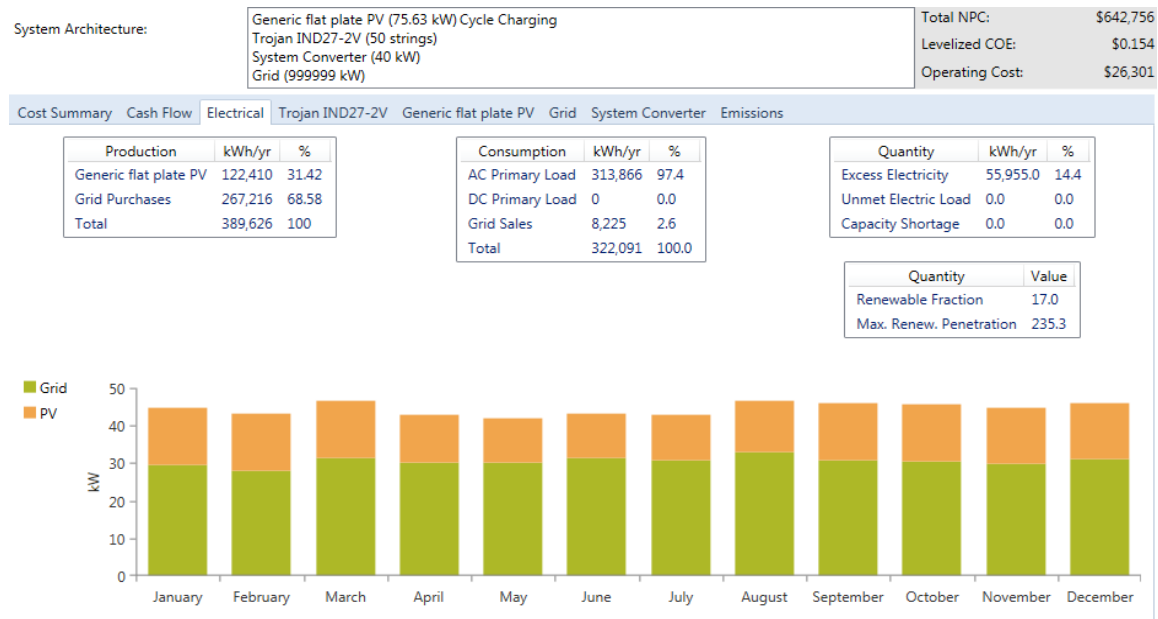


Figure 29: Electrical simulation results for KIST

4.4.6 PV Simulation at KIST

The electrical simulation shows that the rated capacity was 75.63 kW, mean output was 13.974 kW with 335.37 kWh/day, capacity factor was 18.476%, total production was 122 410 kWh/year, maximum output was 73.18 kW, PV penetration was 39.001%, hours of operation was 4338 hours/year and the levelized cost was \$0.187 76/ kWh as shown in Fig. 30.

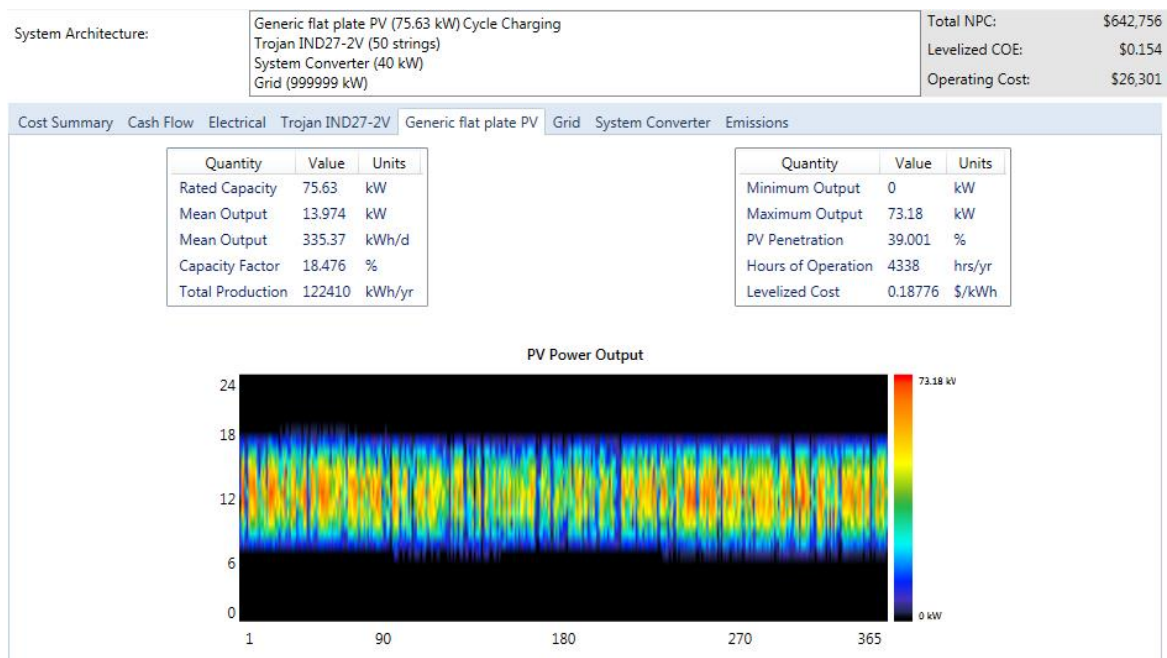


Figure 30: PV simulation results for KIST

4.4.7 Emissions Results for KIST

The emissions results show that the value of carbon dioxide, sulfur dioxide and nitrogen oxides were reduced per year exhibiting 163 682 kg/year, 709.64 kg/year and 347.05 kg/year respectively. Others gas emissions were negligible as shown in Fig. 31.

Quantity	Value	Units
Carbon Dioxide	163,682.00	kg/yr
Carbon Monoxide	0.00	kg/yr
Unburned Hydrocarbons	0.00	kg/yr
Particulate Matter	0.00	kg/yr
Sulfur Dioxide	709.64	kg/yr
Nitrogen Oxides	347.05	kg/yr

Figure 31: Emissions results for KIST

4.5 NM-AIST Simulation Results

The simulation results at NM-AIST shows that sensitivity observed at 0.3 kW PV. The cost of energy (COE), net present cost (NPC), operating cost, initial cost and renewable fraction are \$1.062 /kWh, \$29.169, \$1.931, \$4200 and 22% respectively. Other results for different outputs are as shown in Fig. 32.

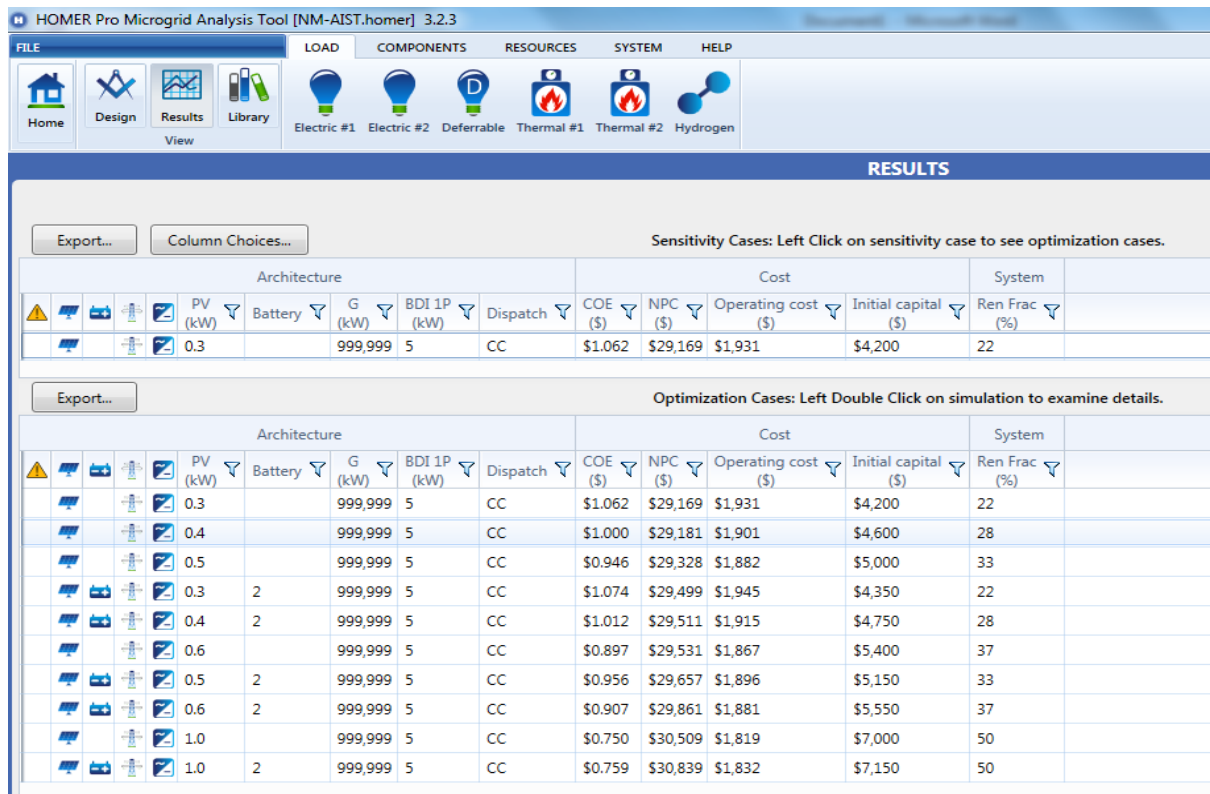


Figure 32: Simulation results for NM-AIST

4.5.1 Cash Summary (Annualized and Net Present) at NM-AIST

The annually and net present cash summary by component results shows that the grid has higher operating costs while the PV modules has higher capital costs as shown in Fig. 33 and 34, respectively.

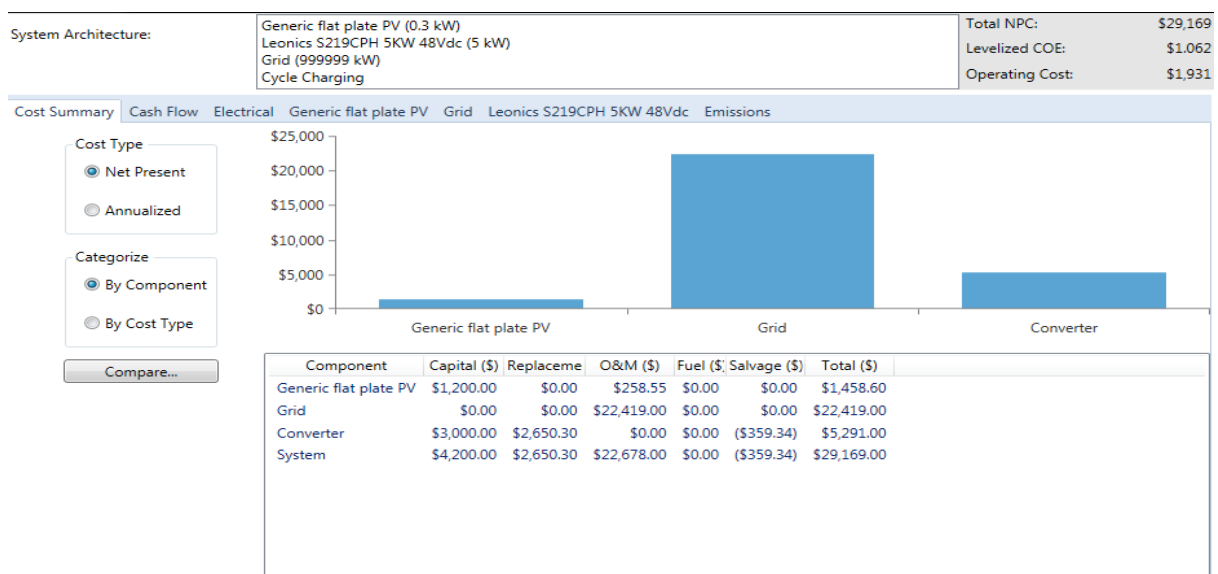


Figure 33: Cost summary (Net present by component) results for NM-AIST

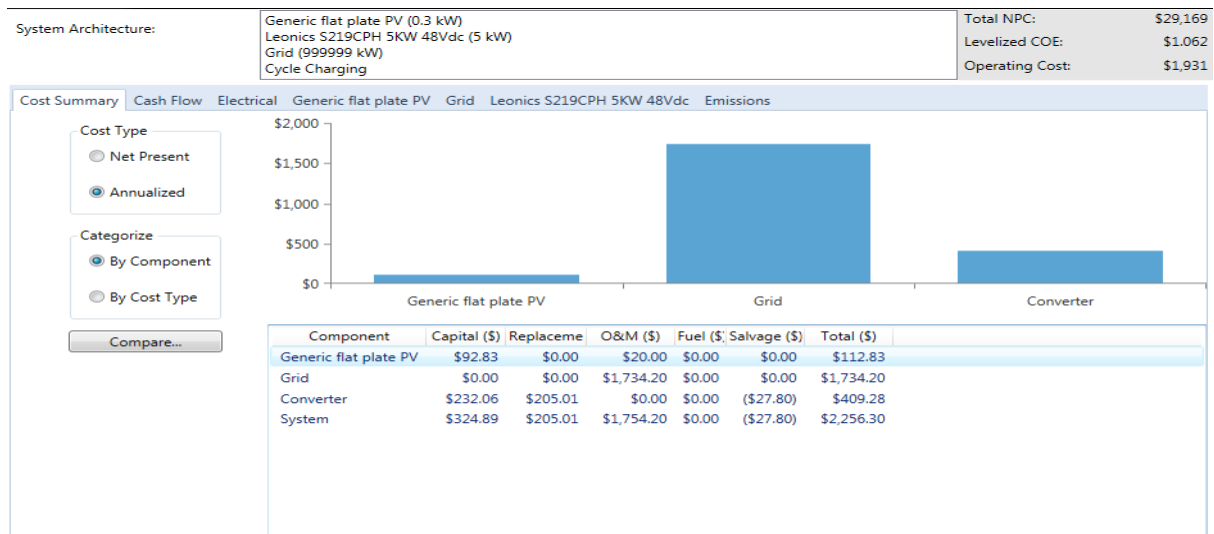


Figure 34: Cost summary (Annualized by component) results for NM-AIST

4.5.2 Cash Summary (Annualized by Cost Type) at NM-AIST

The annually and net present cash summary by cost type results shows that the grid has higher operating costs while the PV modules has higher capital costs as shown in Fig. 35 and 36, respectively.

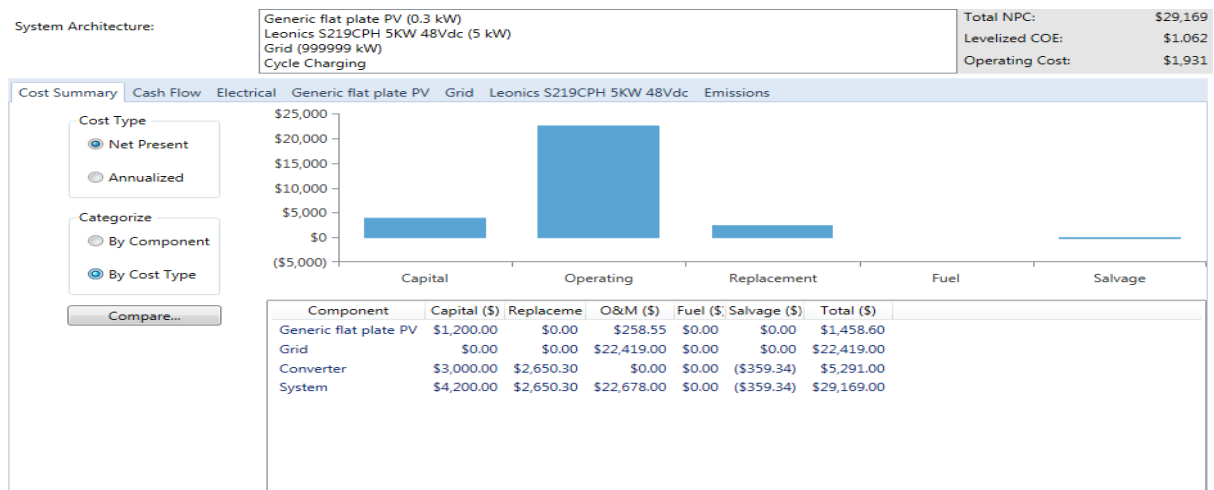


Figure 35: Cost summary (Net present by cost type) results for NM-AIST

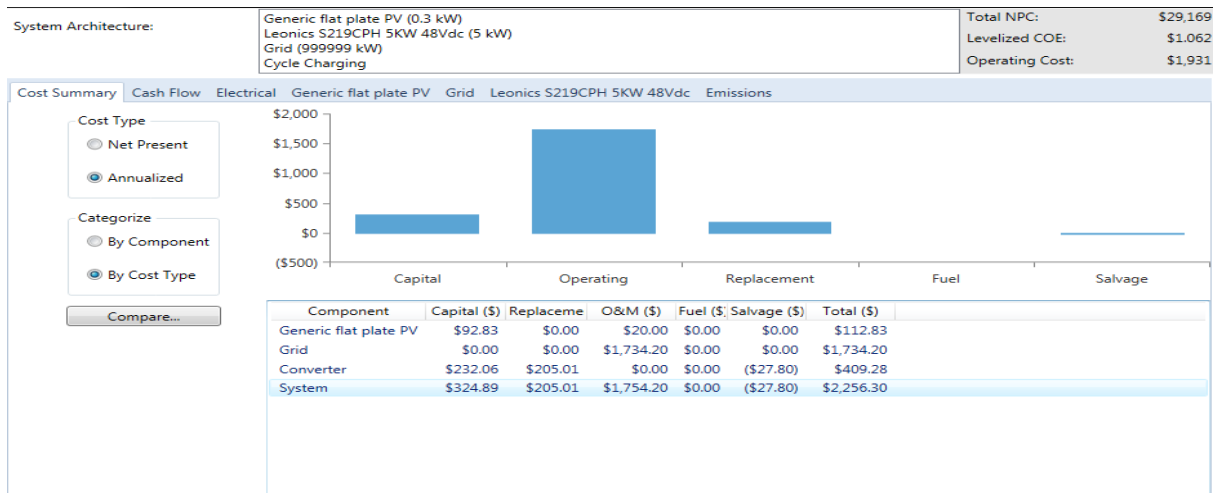


Figure 36: Cost summary (Annualized by cost type) results for NM-AIST

4.5.3 Electrical Simulation at NM-AIST

The electrical simulation shows that the PV modules production was 494 kWh/year and Grid purchase was 1651 kWh/year equivalent to 23.02% and 76.98% of the total production respectively, the consumption rate for AC primary load was 1886 kWh/year and grid sells was 395 kWh/year equivalent to 88.7% and 11.3% of the total consumption respectively. Additionally, the quality value for renewable fraction 22.3 with maximum renewable penetration of 104.2 as shown in Fig. 37.

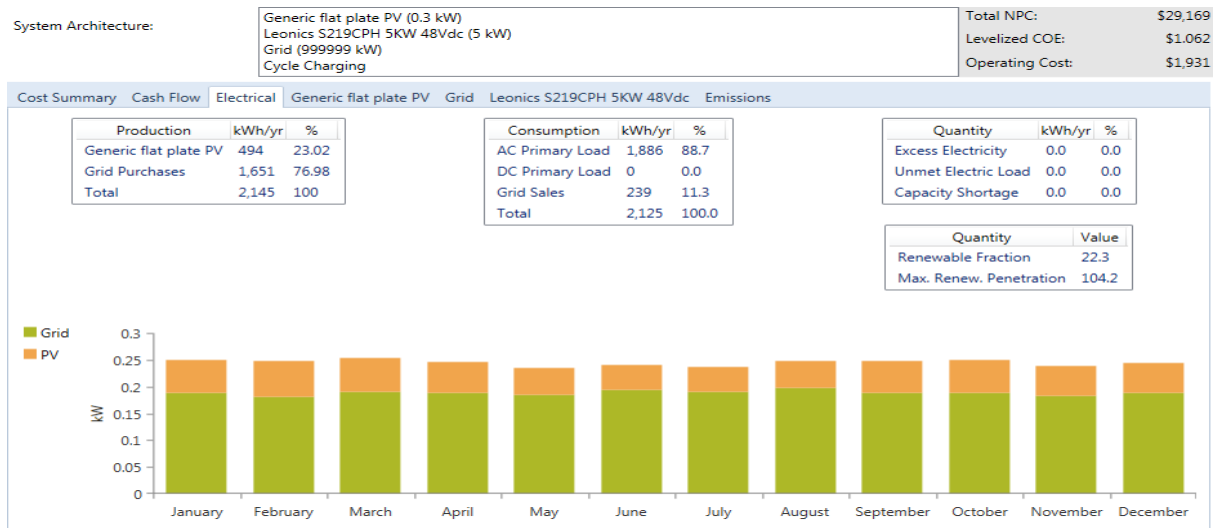


Figure 37: Electrical results for NM-AIST

4.5.4 PV Simulation at NM-AIST

The electrical simulation shows that the rated capacity was 0.3 kW, mean output was 0.056 369 kW with 1.3529 kWh/day, capacity factor was 18.79%, total production was 493.8 kWh/year, maximum output was 0.28 917 kW, PV penetration was 26.184%, hours of operation was 4327 hours/year and the levelized cost was \$0.22 849 /kWh as shown in Fig. 38.

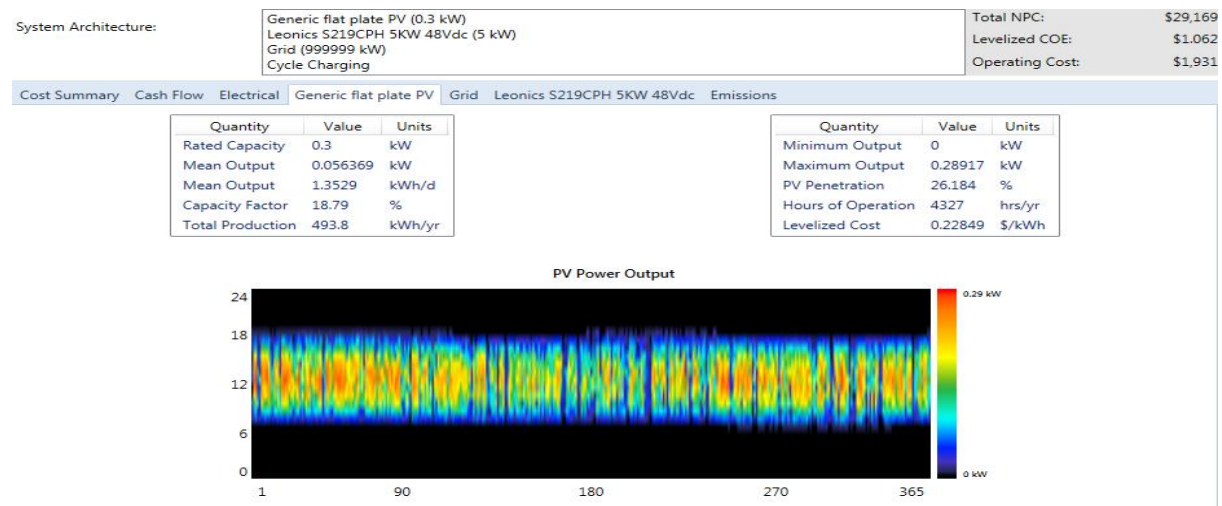


Figure 38: PV results for NM-AIST

4.5.5 Batteries Simulation at NM-AIST

The batteries simulation shows that the rated capacity was 5 kW with rectifier capacity of 4.8 kW, minimum output was 0.054 115 kW, maximum output was 0.2776 kW, capacity factor was 1.0823%, hours of operation was 4326 hours/year, energy output was 474.04 kWh/year and the losses was 19.752 /kWh/year as shown in Fig. 39.

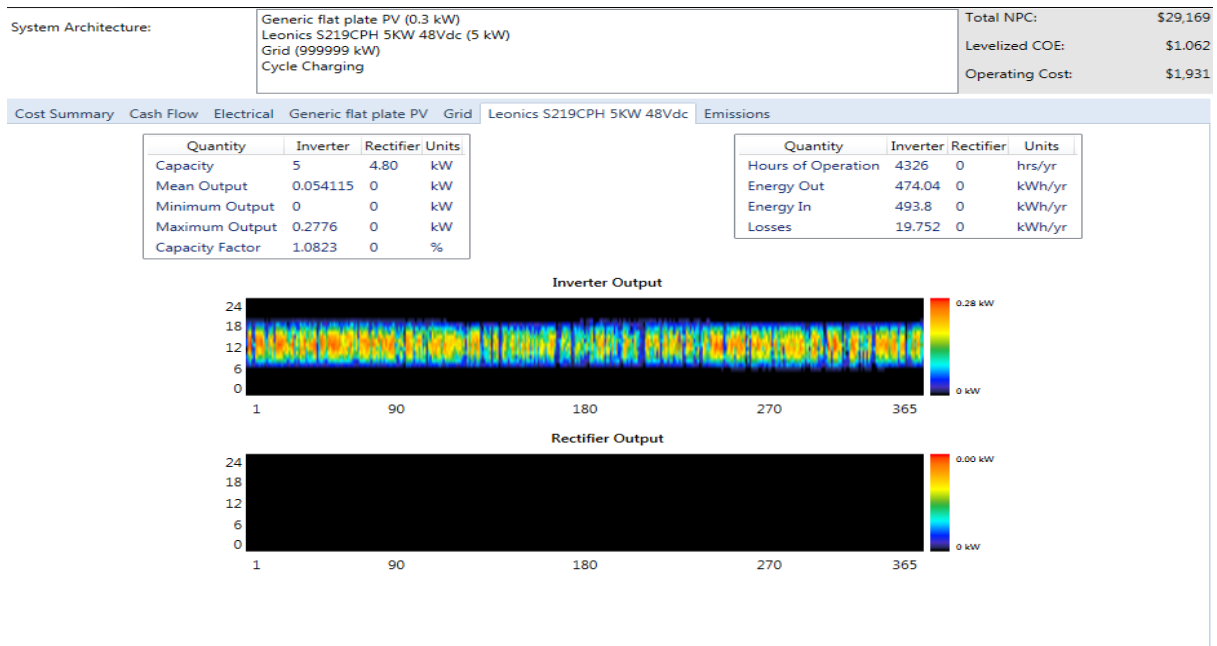


Figure 39: Batteries simulation results for NM-AIST

4.5.6 Grid Simulation at NM-AIST

The grid simulation results show that the higher energy in kWh sold are at the month of January, February and March. Other simulations are shown in Fig. 40.

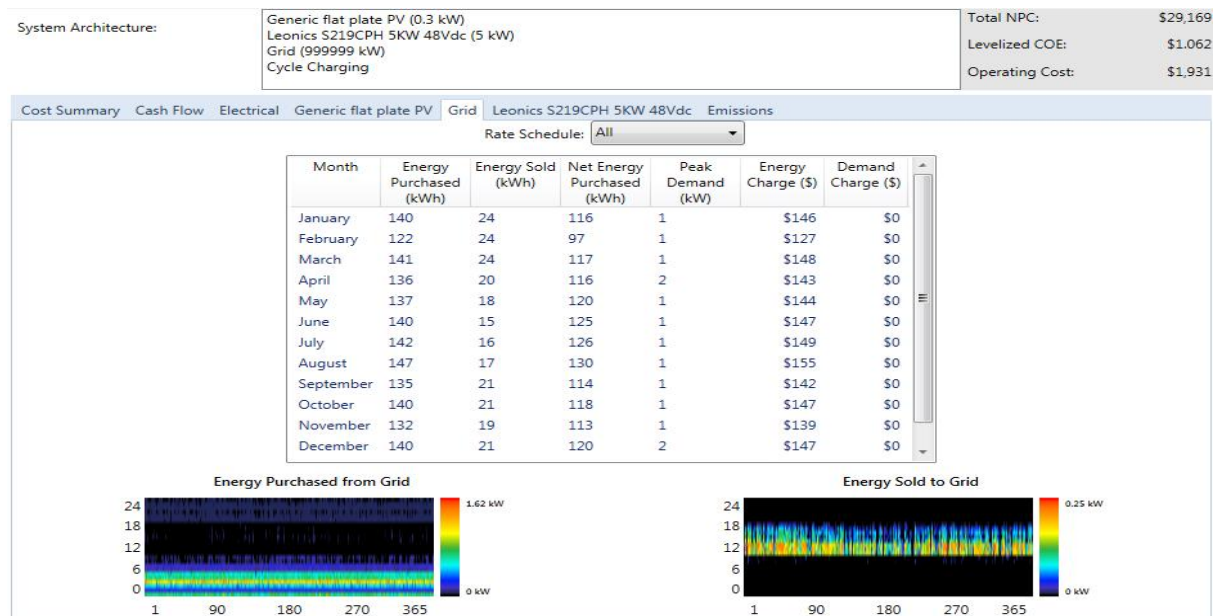


Figure 40: Grid simulation results for NM-AIST

4.5.7 Emissions Results for NM-AIST

The emissions results show that the value of carbon dioxide, sulfur dioxide and nitrogen oxides reduced per year were 892.29 kg, 3.87 kg and 1.89 kg respectively. Others gas are as shown in Fig. 41.

Quantity	Value	Units
Carbon Dioxide	892.29	kg/yr
Carbon Monoxide	0.00	kg/yr
Unburned Hydrocarbons	0.00	kg/yr
Particulate Matter	0.00	kg/yr
Sulfur Dioxide	3.87	kg/yr
Nitrogen Oxides	1.89	kg/yr

Figure 41: Emissions results for NM-AIST

4.5.8 Daily Load (July 2017)

The daily load for the month of July shows that 4th July has high load loads as shown in Fig. 42.

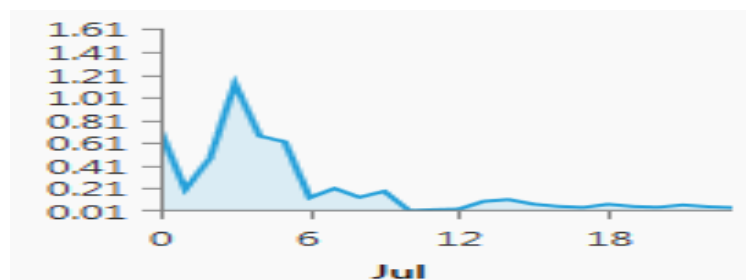


Figure 42: July 2017 load curves results for NM-AIST

4.5.9 Total Renewable Power Output

The renewable power output for the month of June and July is shown in Fig. 43 .

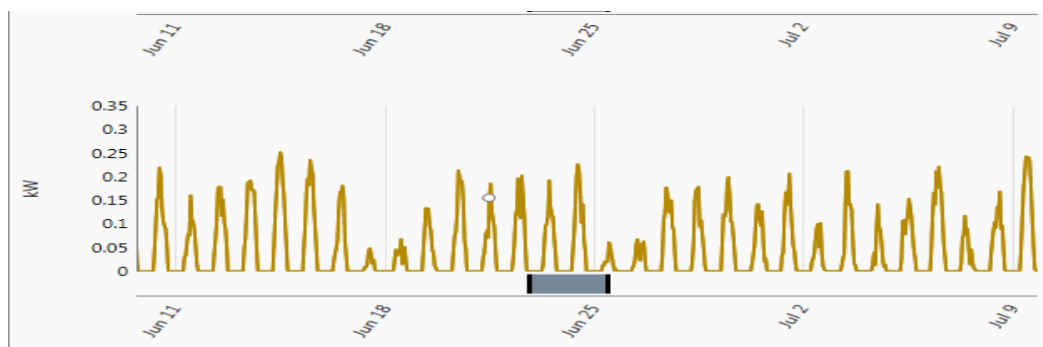


Figure 43: Hourly renewable power output results for NM-AIST

The economic, system control, emission and constraints for the systems are shown in Table 9.

Table 9: Economics, system control, emission and constraints

Description	Quality	KIST	NM-AIST
Economics	Annual real interest rate	6%	6%
	Project lifetime	25 years	25 years
	Capacity shortage penalty	\$0/kWh	\$0/kWh
	System fixed capital cost	0	0
	System fixed O&M cost	0	0
System control	Check load following	No	No
	Check cycle charging	Yes	Yes
	Set point state of charge	80	80
	Allow systems with multiple generators	Yes	Yes
	Allow multiple generators to operate simultaneously	Yes	Yes
	Allow systems with generator capacity less than peak load	Yes	Yes
Emission	Carbon dioxide penalty	\$ 0/t	\$ 0/t
	Carbon monoxide penalty	\$ 0/t	\$ 0/t
	Unburned hydrocarbons penalty	\$ 0/t	\$ 0/t
	Particulate matter penalty	\$ 0/t	\$ 0/t
	Sulfur dioxide penalty	\$ 0/t	\$ 0/t
	Nitrogen oxides penalty	\$ 0/t	\$ 0/t
Constraints	Maximum annual capacity shortage	1	0
	Minimum renewable fraction	0	0
	Operating reserve as percentage of hourly load	10	10
	Operating reserve as percentage of peak load	0	0
	Operating reserve as percentage of solar power output	25	25
	Operating reserve as percentage of wind power output	50	50

CHAPTER FIVE

CONCLUSION AND RECOMMENDATIONS

5.1 Conclusion

This research work presents the simulation and performance analysis of a solar photovoltaic (PV) at KIST and NM-AIST. Studies were carried out experimentally and simulations using the HOMER software. Performance of the experimentally Solar PV intended that the distance from the roof to the panel, reflection and inclination angles have significant impact on the performance of PV panels. The high performance was obtained when the distance from the roof to the panel was 20 cm and the reflection and inclination angles were 45° and 20° respectively. The spacing provided good natural cooling of the panel while at the optimal reflection and inclination angles the solar intensity was improved due to the decreased angle of incidence.

Analysis reveal that the PV systems have the lowest net present cost (NPC) are carried out to determine the break-even grid extension distance from the system locations. It is observed that when the system is connected to the external grid, it is the most economical option because of the fact that there is no capital cost involved, and its operation and maintenance costs are much less compared to the grid system only. In addition, it is more environmentally friendly because of the significant reduction in system emissions. However, the system has high initial capital and replacement costs.

This work also demonstrated that allowing a small amount of annual load to be left unmet makes the systems more cost-effective. Finally, the break-even distance presented in this work shows that for isolated system, far away from the external grid connectivity point is the most economic optimal choice. It is observed that the NPC and the levelized cost of energy reduces somewhat, when allowable unmet resources as far as possible even when the unmet energy margin.

5.2 Recommendations

In reality, the economic performance of the system was found to be very sensitive to fuel cost and price, specific risk factors significantly reduced system profitability with increasing of energy efficiency. The technical, economic and policy risks are implemented to increase the probability of economic viability. Tanzanian reflection is best to do this for energy efficiency and good results for having solar energy that will provide access to energy for the whole

period. It is also suggested that to have backup batteries for accessing the energy for 24 hours a day.

REFERENCES

- Al-Messabi, N., Goh, C. and Li, Y. (2016). Heuristic grey-box modelling for photovoltaic power systems. *Systems Science and Control Engineering*, 4(1), 235-246.
- Ani, V. A. and Abubakar, B. (2015). Feasibility Analysis and Simulation of Integrated Renewable Energy System for Power Generation: A Hypothetical Study of Rural Health Clinic. *Journal of Energy*, 2015.
- Anwari, M., Rashid, M. I. M., Hui, H .I., Yee, T. W. and Wee, C. K. (2011). *Photovoltaic power system simulation for small industry area*. Paper presented at the Electrical, Control and Computer Engineering (INECCE), 2011 International Conference on.
- Bank, The World. (2015). *Renewable Energy Resource Mapping. Solar Tanzania*. Paper presented at the Energy Sector Management Assistance Program, 1818 H Street, NW. USA. Washington, DC 20433.
- Bernal, A., José, L. and Dufo-Lopez, R. (2009). Simulation and optimization of stand-alone hybrid renewable energy systems. *Renewable and Sustainable Energy Reviews*, 13(8), 2111-2118.
- Bull, S. R. (2001). Renewable energy today and tomorrow. *Proceedings of the IEEE*, 89(8), 1216-1226.
- Cogeneration Biomass-Based, Gwang'ombe, F. R. D. and Salaam, D. (2004). Renewable Energy Technologies in Tanzania.
- Couture, T. and Gagnon, Y. (2010). An analysis of feed-in tariff remuneration models: Implications for renewable energy investment. *Energy policy*, 38(2), 955-965.
- Ellabban, O., Abu-Rub, H. and Blaabjerg, F. (2014). Renewable energy resources: Current status, future prospects and their enabling technology. *Renewable and Sustainable Energy Reviews*, 39, 748-764.
- Gupta, A. and Srinivasa, V. U. (2012). Design, simulation and verification of generalized photovoltaic cells model using first principles modeling. *ACEEE International Journal on Control System and Instrumentation*, 3(01), 11-17.

- Gwang'ombe, F. and Mwiha, N. (2005). Renewable in Tanzania: Status and Prospects of Biomass Based Cogeneration and Geothermal Technologies. HBF-HA, Sida/SAREC and AFREPREN/FWD.
- Hammer, A., Heinemann, D., Hoyer, C., Kuhlemann, R., Lorenz, E., Müller, R. and Beyer, H.G. (2003). Solar energy assessment using remote sensing technologies. *Remote Sensing of Environment*, 86(3), 423-432.
- Herscovitz, A. M. and Pielli, K. (2016). Driving Renewable Energy in sub-Saharan Africa through Public-Private Cooperation. *World Economic Forum*.
- Ishaque, K., Salam, Z., Mekhilef, S. and Shamsudin, A. (2012). Parameter extraction of solar photovoltaic modules using penalty-based differential evolution. *Applied Energy*, 99, 297-308.
- Limmanee, A., Songtra, S., Udomdachanut, N., Kaewniyompanit, S., Sato, Y., Nakaishi, M. and Sakamoto, Y. (2017). Degradation analysis of photovoltaic modules under tropical climatic conditions and its impacts on LCOE. *Renewable Energy*, 102, 199-204.
- Liu, G., Rasul, M. G., Amanullah, M. T. O. and Khan, M. M. K. (2012). Techno-economic simulation and optimization of residential grid-connected PV system for the Queensland climate. *Renewable Energy*, 45, 146-155.
- Marion, B., Adelstein, J., Boyle, K., Hayden, H., Hammond, B., Fletcher, T. and Mitchell, L. (2005). *Performance parameters for grid-connected PV systems*. Paper presented at the Photovoltaic Specialists Conference, 2005. Conference Record of the Thirty-first IEEE.
- Mishra, S., Panigrahi, C. K. and Kothari, D. P. (2016). Design and simulation of a solar–wind–biogas hybrid system architecture using HOMER in India. *International Journal of Ambient Energy*, 37(2), 184-191.
- Mohammed, Y. S., Mustafa, M. W. N., Bashir, N. and Mokhtar, A. S. (2013). Renewable energy resources for distributed power generation in Nigeria: a review of the potential. *Renewable and Sustainable Energy Reviews*, 22, 257-268.

- Nair, N. C. and Garimella, N. (2010). Battery energy storage systems: Assessment for small-scale renewable energy integration. *Energy and Buildings*, 42(11), 2124-2130.
- Okello, D, Van, D. E. E. and Vorster, F. J. (2015). Analysis of measured and simulated performance data of a 3.2 kWp grid-connected PV system in Port Elizabeth, South Africa. *Energy conversion and management*, 100, 10-15.
- Parida, B., Iniyar, S. and Goic, R. (2011). A review of solar photovoltaic technologies. *Renewable and sustainable energy reviews*, 15(3), 1625-1636.
- Ramli, M. A. M, Hiendro, A., Sedraoui, K. and Twaha, S. (2015). Optimal sizing of grid-connected photovoltaic energy system in Saudi Arabia. *Renewable Energy*, 75, 489-495.
- Saidur, R., BoroumandJazi, G., Mekhlif, S. and Jameel, M. (2012). Exergy analysis of solar energy applications. *Renewable and Sustainable Energy Reviews*, 16(1), 350-356.
- Sharma, R. and Goel, S. (2017). Performance analysis of a 11.2 kWp roof top grid-connected PV system in Eastern India. *Energy Reports*, 3, 76-84.
- Shukla, A. K., Sudhakar, K. and Baredar, P. (2016). Simulation and performance analysis of 110 kW p grid-connected photovoltaic system for residential building in India: a comparative analysis of various PV technology. *Energy Reports*, 2, 82-88.
- Yang, H. X., Lu, L. and Burnett, J. (2003). Weather data and probability analysis of hybrid photovoltaic–wind power generation systems in Hong Kong. *Renewable Energy*, 28(11), 1813-1824.

APPENDICES

Appendix 1: Standalone measurement for solar PV in KIST

EXPERIMENTAL CONDITION	PARAMETERS	I _{sc} [A]	V _{oc} [V]	P[W]
Reference	30°, <10 cm and without reflector	3.93	39.29	153.66
Angle of inclination	0°	2.77	39.12	147.48
	10°	1.40	38.46	133.07
	20°	4.00	38.89	155.56
	40°	2.52	38.80	137.88
Distance from the roof	10 cm	2.77	39.12	149.05
	15 cm	1.97	38.00	139.46
	20 cm	4.01	38.89	155.95
	25 cm	2.78	38.89	147.00
Using reflector	45°	3.98	39.12	155.70
	50°	3.40	38.46	130.76
	55°	3.76	38.89	146.23
	60°	3.52	38.80	136.58

Appendix 2: Grid connected measurement parameters at KIST

Month	D.C Values				A.C Values			
	I[A]	V[V]	P[W]	E[Wh]	I[A]	V[V]	P[W]	E[Wh]
JAN	11.64	442.30	5148.37	52 770.81	17.21	243.67	4193.56	42 984.00
FEB	11.45	418.56	4792.51	49 123.25	17.23	242.45	4177.41	42 818.49
MAR	10.34	411.43	4254.19	43 605.41	16.98	243.98	4142.78	42 463.50
APR	9.02	421.34	3800.49	38 954.99	14.39	244.12	3512.89	36 007.09
MAY	8.84	402.70	3559.87	36 488.65	14.76	222.43	3283.07	33 651.43
JUN	9.75	442.10	4310.48	44 182.37	15.61	244.51	3816.80	39 122.21
JUL	11.02	443.26	4884.73	50 068.43	17.58	241.98	4254.01	43 603.59
AUG	11.75	412.30	4844.53	49 656.38	17.76	241.73	4293.12	44 004.53
SEP	12.12	431.50	5229.78	53 605.25	17.97	228.74	4110.46	42 132.19
OCT	12.50	421.45	5268.13	53 998.28	17.23	231.56	3989.78	40 895.23
NOV	12.67	414.48	5251.46	53 827.48	18.12	229.85	4164.88	42 690.04
DEC	12.83	426.97	5478.03	56 149.76	18.43	228.78	4216.42	43 218.26

RESEARCH OUTPUTS

Output 1: Paper Presentation

American Journal of Electrical Power and Energy Systems

2019; 8(1): 11-22

<http://www.sciencepublishinggroup.com/j/epes>

doi: 10.11648/j.epes.20190801.12

ISSN: 2326-912X (Print); ISSN: 2326-9200 (Online)



Performance Analysis of Installed Solar PV System Using Homer in Tanzania: A Case Study of Zanzibar and Arusha

Mohammed Haji^{*}, Eugene Park, Thomas Kivevele

Department of Materials, Energy Science and Engineering, The Nelson Mandela African Institution of Science and Technology (NM-AIST), Arusha, Tanzania

Email address:

edimhaji@live.com (M. Haji), eugene.park@nm-aist.ac.tz (E. Park), thomas.kivevele@nm-aist.ac.tz (T. Kivevele)

^{*}Corresponding author

To cite this article:

Mohammed Haji, Eugene Park, Thomas Kivevele. Performance Analysis of Installed Solar PV System Using Homer in Tanzania: A Case Study of Zanzibar and Arusha. *American Journal of Electrical Power and Energy Systems*. Vol. 8, No. 1, 2019, pp. 11-22.
doi: 10.11648/j.epes.20190801.12

Received: November 4, 2018; **Accepted:** February 7, 2019; **Published:** March 6, 2019

Abstract: This study reflects two photovoltaic (PV) power generations, at Karume Institute of Science and Technology (KIST) - Zanzibar and The Nelson Mandela African Institution of Science and Technology (NM-AIST) - Arusha in Tanzania. The output data sets from each site were verified for possible PV simulation of different operational scenarios to obtain the optimum design configuration. The HOMER software was used to analyze the entire operation of the system. The effect of the accuracy of the photovoltaic integration was determined by analysis of different operational behaviors of the simulated PV levels. Furthermore, the overall performance of the station per site was analyzed for technical, economic and environmental constraints as well as their comparative cost-benefit analysis. The study finds that there is a high sensitivity in the demand for the load (i.e. load growth) whose system performance is characterized with minimum: total net present cost (NPC) of \$474,745 and \$29,169, feed in tariffs, levelized cost of energy (LCOE) of \$1.06/kWh and \$0.0118/kWh, total energy output and renewable fraction of 15% and 22% for KIST and NM-AIST respectively, thus support the use of photovoltaic power sources in the generation of energy than their counterpart alternatives because of the best technical performance and is less dependent on other external sources of energy, and simultaneously has good economic and environmental performance

Keywords: Solar PV System, Performance, Analysis, HOMER, Economic Simulation

1. Introduction

Renewable energy is the energy that is not depleted as it is continuously replenished when utilized. This includes solar energy, wind energy, hydro and geothermal energy. Solar PV is derived from the conversion of sunlight to electrical energy using photovoltaic cells. The electrical energy generated can be used in off grid power system or supplied to the main grid when it reaches substantial amounts. This feature makes Solar PV one of the most important renewable energy sources that will potentially contribute significantly to the energy deficit in Tanzania [1].

The utilization of Solar PV as the source of energy will certainly minimize greenhouse gases emissions and adverse climate changes which world is currently experiencing such as droughts and loss of species diversity on planet. Solar PV seem to be a more promising renewable energy source due to

frequency of sunlight radiation the country receives throughout the year [2]. The frequency of sunlight and the geographical position of Tanzania across the equator make solar energy to be an ideal renewable source of energy, which will substitute the use of fossils fuels in the country. However, measuring the performance of Solar PV system in order to determine the potential of the solar PV utilization and optimization in Tanzania is the focus of this paper.

Renewable energy therefore will ensure and facilitate the development of clean energy development as well as the national sustainable energy development agendas [3].

Decline in reserve and drastically rise of price of fossil fuels as well as their impacts on the world climate change due to exceedingly greenhouse gases emission [4]. The situation has made Tanzania to strategically planning to employ the use of renewable energy particularly the solar PV and hydroelectric power.

HOMER Software

The performance and improvement on any solar systems differs from one geographical location to another and the component features of the solar panel as described by the Hybrid Optimization Modeling for Electric Renewable (HOMER) software. The HOMER software performs: energy balance calculations, system cost calculations for each system configuration, listing of all the possible system sizes, and sorts them by Net Present Cost (NPC). HOMER is made of several energy components, and is used to evaluate suitable options for considering cost against availability of energy resources [5].

The HOMER design procedure is a major consideration when making Grid connections, - where initial information namely energy resources, possible economic and technical constraints, energy storage requirements and control strategies of the systems are accounted for beforehand. Other essential inputs considered include component type, operation, capital, replacement and maintenance costs, efficiency and operational life. Besides being required in the grid connection, the aforementioned inputs are also vital in the stand-alone systems, and are applicable in both installed energy sources and conventional systems [6].

Most of the demonstration and experimentation of the PV systems, as alternative sources of renewable energy focus on installation will be minimal, if any, investigation given to study the feasibility and optimal combination of resources. Several constraints in line with feasibility and optimal resource allocation have resulted into failures in meeting the required load demand and related economic sustainability.

A case study of the application of the HOMER software is by Bernal-Aguistin and Dufo-Lopez [7], used it for Optimization and Simulation of Solar Photovoltaic cell in a residential building in Malviya Nagar, India. The optimization of the solar photovoltaic cell on the residential building, which had a total roof area of 576 m² and had 16 flats, was done using HOMER software. The average solar radiation data of the location as well as the cost of the different component required for the setup was observed. The optimization output was 160 kW PV cell which was required at a cost of \$0.184 for electricity generation.

Conversely, Anwari, Rashid [8] presented a photovoltaic power system simulation for small industry area in Malacca, Malaysia. The modeling and simulation of 1 MW grid connected PV system was simulated using the National Renewable Energy Laboratory's (NREL) HOMER software, and the optimum system was analyzed for the economic feasibility. The system was expected to foresee reduced grid energy consumption while simultaneously reduce greenhouse gases emissions. The HOMER software simulated the system and performance optimization of system was done using both secondary usage data and the renewable solar radiation data. Results indicated that both the lifecycle and cost of each system modules duly affected the optimization and confirmed the significant efficiency of the proposed approach to the development of renewable energy systems with PV power generators.

In a dissimilar scenario, Ani and Abubakar [9] calculated feasibility analysis and simulation of integrated renewable energy system for power generation in his hypothetical study of integrated renewable energy (IRE) in rural health clinic in Borno State in Nigeria, using solar photovoltaic (PV) and wind turbine (WT) systems. The results indicated that the energy output from the integrated systems was suitable for deployment of 100% clean energy for uninterruptable power supply with optimum performance in the health clinic. It was concluded that, with a low energy health facility, it is possible to meet the entire annual energy demand of a health clinic solely through a stand-alone integrated renewable PV/wind energy supply without grid-connection.

Besides, the performance of the integrated system on the grid-tied connection needs to be assessed. This includes evaluating the implication of the grid-connected PV system to the total power output of the systems as well as the PV generation on the entire system. The key factors to consider are the: sensitivity and the suitability in enhancing the overall output, feasibility factors, cost-effectiveness, data provision on PV system under grid connection, the system optimization parameters to the consumer etc [10].

This study, therefore, evaluates and analyzes the performance of grid-connected solar PV of 75.63kW_p and 0.3kW_p at Karume Institute of Science and Technology and Nelson Mandela African Institution of Science and Technology respectively.

2. Methodology

The instrument used in this study were multimeter (model INNOVA 3300), for measuring short circuits currents and open circuit voltages of the PV modules. The short-circuit current (I_{sc}) is the current through the solar PV when the voltage across the solar cell is zero (i.e., when the solar PV is short-circuited) and the open-circuit voltage, V_{oc} , is the maximum voltage available from a solar cell, and this occurs at zero current.

Because any successful evaluation requires proper application of prerequisite standards on site data to facilitate correct analysis of the operational behavior of all possible scenarios, the following analysis framework for site specification, verification of demonstrated data sets (i.e., solar energy, solar insolation and load demand), system analysis and operational performance impact were employed.

2.1. Site Specifications

KIST is located at the latitude -6.16 (6°09'36"S), longitude +39.2 (39°12'00"E) and altitude 0 m at a distance of 72 km above the Indian Ocean while NM-AIST is located at the latitude -3.4 (3°24'0"S), longitude +36.78 (36°47'8"E) Arusha region on north of Tanzania.

2.2. Technical Data

Solar panels are rated to perform according to their specifications under standard test conditions (STC) - a

condition that can be created in a lab to allow easy measurement and comparison. The defined STC for solar is a panel pointed directly at a bright sun with 1000W of solar energy landing per square meter, with the panel kept at 25°C

(77 °F) and an atmospheric mass (a number that refers to the amount of atmosphere between the panel and the sun) of 1.5 overhead. Table 1 illustrates technical details for the existing system and the module specifications are shown in Table 2.

Table 1. Technical detail of the systems.

Designation	KIST Administration	KIST dining hall	NM-AIST
Power	25.21 kW _p	50.42 kW _p	0.3 kW _p
Area	176.94 m ²	353.88 m ²	4.07 m ²
Tracking system	Without tracking system		
Tilt	30°		
Orientation	0°		
Type of installation	Roof top installation, small distance (<10 cm)		>10 cm
System start-up	31/10/2013		2017
Series-connected	15	15	2
Parallel-connected	2	2	2
Inverter type	SMA SMC 8000TL		WINKLE POWER
Number of inverters	3	6	1
Module type	Hamwha SF260 Poly (280 W)		Si-3000S
Number of modules	90	180	4

Table 2. PV module specifications.

Quantity	Symbol	Unit	KIST Values		NM-AIST Values	
			STC	NOCT	STC	NOCT
Maximum power rating	P _{max}	W	280	204	150	108
Open circuit voltage	V _{oc}	V	44.3	40.8	22.19	20.2
Short-circuit current	I _{sc}	A	8.45	6.84	8.62	6.9
Rated voltage at max. power	V _{mp}	V	36.2	32.9	18.16	16.2
Rated current at max. power	I _{mp}	A	7.87	6.21	8.06	6.7
Module efficiency	H	%	14.3		14.88	
Weight	W	Kg	11.6		12	
Dimensions	-	mm	1483*668*35		1510*674*50	
Maximum system voltage	V _{max}	V _{DC}	1000			
Wind resistance	-	P _s	2400			

2.3. Current and Voltage Measurements of the Solar PV Systems

The open-circuit voltage (V_{oc}) and the short-circuit current (I_{sc}) cannot be measured at the same time because they correspond to different operating modes of the device. At open-circuit, which is the case a voltmeter with a high input impedance (several Mega-ohms) was connected to solar PV, the excess carriers cannot leave the device with the result that the external current is zero. Subsequently, all carriers are forced to recombine and the recombination rate equals the generation rate under steady state conditions [11].

In a grid connected, the current was measured by using a coil wound round the PV inductor and connect the coil to the second data logger channel to measure the output voltage on the coil. These measurements were taken under the tag energy meter per day from 7:15 to 17:30 hours and their average values in each month. Table 3 shows grid connected system parameters at KIST.

Table 3. Grid connected measurement parameters at KIST.

Month	D. C Values		A. C Values	
	I [A]	V [V]	I [A]	V [V]
JAN	11.64	442.30	17.21	243.67
FEB	11.45	418.56	17.23	242.45
MAR	10.34	411.43	16.98	243.98
APR	9.02	421.34	14.39	244.12
MAY	8.84	402.70	14.76	222.43
JUN	9.75	442.10	15.61	244.51
JUL	11.02	443.26	17.58	241.98
AUG	11.75	412.30	17.76	241.73
SEP	12.12	431.50	17.97	228.74
OCT	12.50	421.45	17.23	231.56
NOV	12.67	414.48	18.12	229.85
DEC	12.83	426.97	18.43	228.78

The d.c voltage current and power measurements for NM-AIST system is represented in Table 4 as recorded from the data logger

Table 4. Measurements taken from solar PV in NM-AIST.

CURRENT (A)	BATTERY VOLTAGE (V)	NORTH VOLTAGES (V)	SOUTH VOLTAGES (V)	TOTAL VOLTAGES (V)	POWER (W)
24.81	28.95	25.78	25.97	28.53	707.84
6.87	28.9	25.57	25.92	28.53	196.08
18.58	28.9	25.57	25.8	25.24	468.82
39.35	28.95	25.53	25.75	28.14	1107.13
24.9	28.95	25.57	25.75	27.08	674.15
24.71	28.95	25.66	25.8	24.4	602.92
4.56	28.95	25.57	25.75	28.53	130.04
7.39	28.95	25.57	25.75	28.53	210.74
4.74	28.95	25.57	25.88	26.91	127.6
6.5	28.95	25.57	25.88	28.53	185.45
0.55	28.9	25.57	25.71	26.52	14.58
0.89	28.9	25.57	25.84	26.44	23.42
1.05	28.9	25.66	25.8	26.46	27.89
3.58	28.9	25.57	25.75	26.27	94.09
4.17	28.9	25.57	25.8	26.38	110.1
2.7	28.9	25.57	25.75	26.44	71.32
1.96	28.9	25.57	25.8	26.44	51.81
1.59	28.9	25.57	25.88	26.44	42.06
2.69	28.95	25.66	25.8	26.32	70.8
1.96	28.95	25.61	25.88	26.49	51.81
1.65	28.9	25.57	25.75	26.38	43.52
2.47	28.9	25.57	25.88	26.38	65.28
1.85	28.9	25.57	25.88	26.44	48.86

2.4. The Existing PV System

An electrical grid is an interconnected network for delivering electricity from suppliers to consumers and investigated in the present study is shown in the Figure 1.



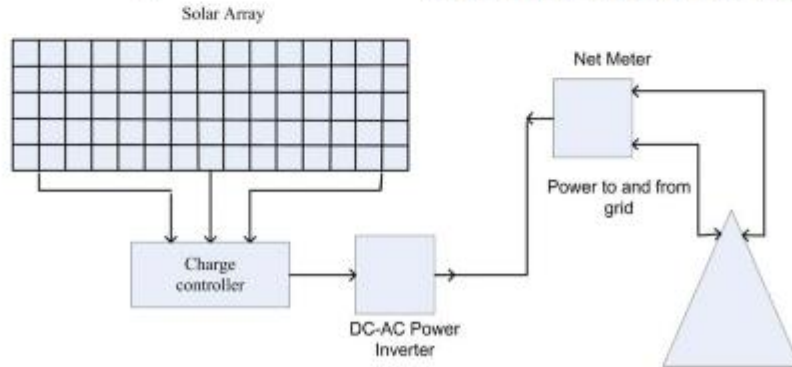
(a)



(b)

Figure 1. PV system (a) PV system at KIST (b) PV system at NM-AIST.

The existing block diagram for the systems are as shown in Figure 2 and Figure 3 for KIST and NM-AIST respectively.

**Figure 2.** Block diagram of KIST PV system.

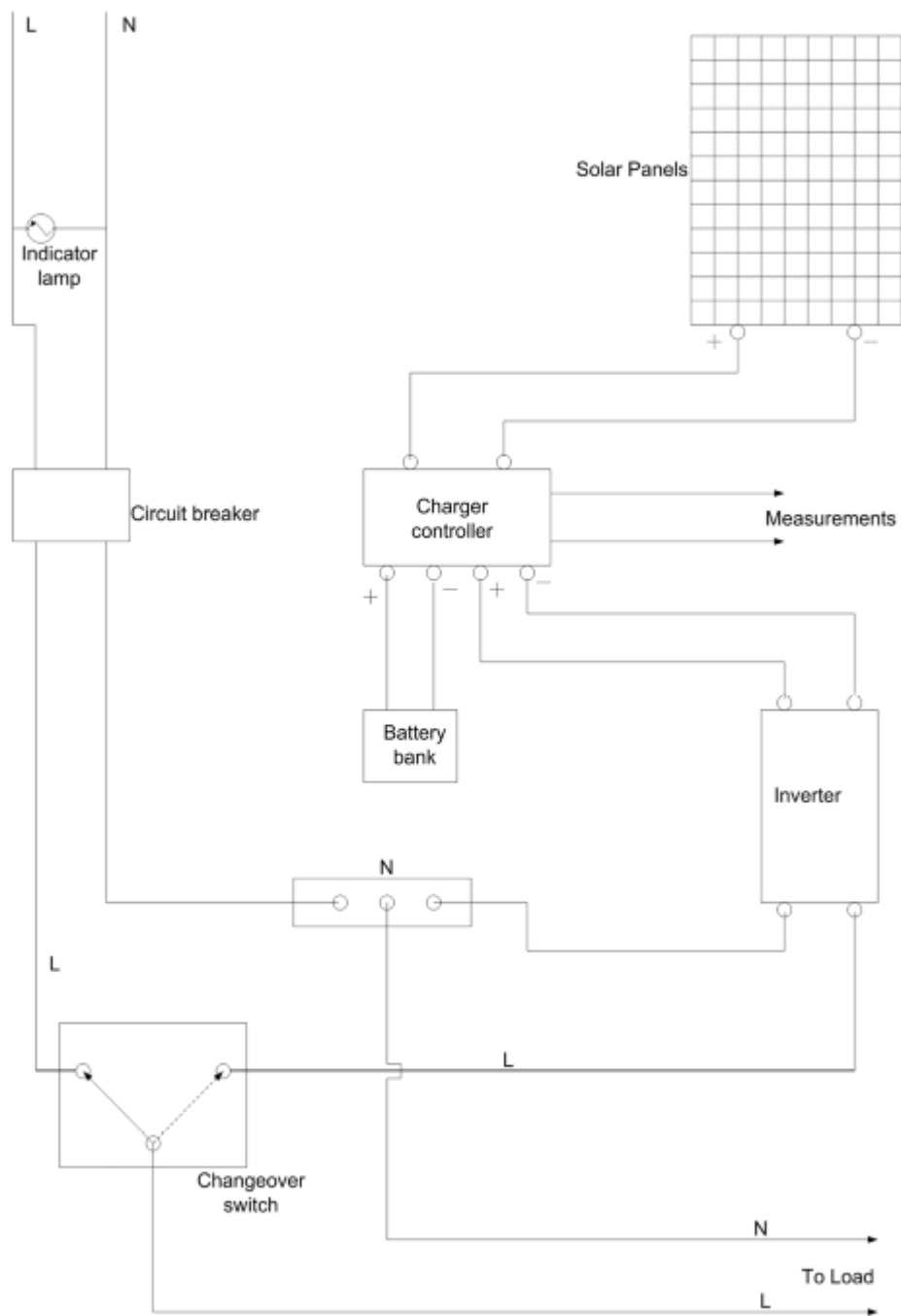
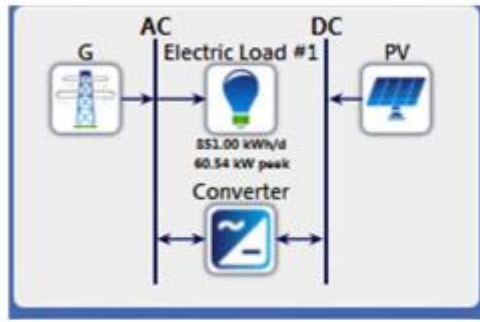


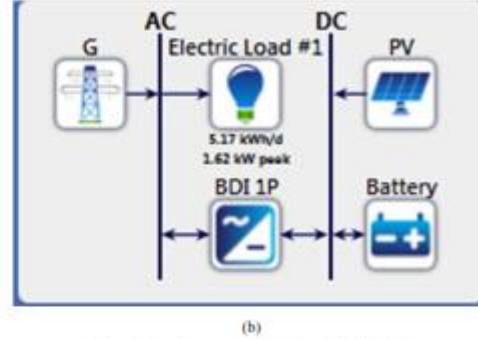
Figure 3. NM-AIST PV System arrangement.

2.5. Data Verifications and System Configuration

The system data parameters taken were solar radiation, ambient temperature, load profile and demand data as shown in Figure 4 and 5. The real-time measurement of solar irradiation and ambient temperature data was done in order to assess the optimum performance of the system. However, due to the internal limitations within the system namely faulty sensors and measuring tools, the measured data was limited. Nonetheless, the missing data was compensated by that obtained from National Aeronautics and Space Administration (NASA), - which was used as another input data.



(a)

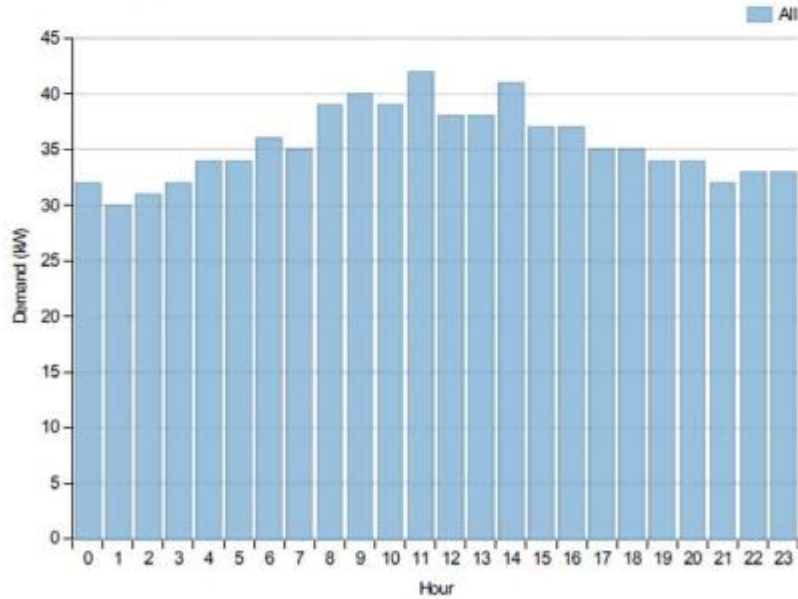


(b)

Figure 4. Configuration (a) KIST and (b) NM-AIST.

2.6. Solar Resource

Solar insolation data obtained from NASA's website, in the event of unavailability of sufficient measured data in the desired locations [12]. Monthly solar insolation data for both locations are generally in the range of 4.3 – 6.52 kWh/m²/day, with an annual average of 5.39 and 5.58 kWh/m²/day for NM-AIST and KIST respectively as presented in Table 5.



(a)

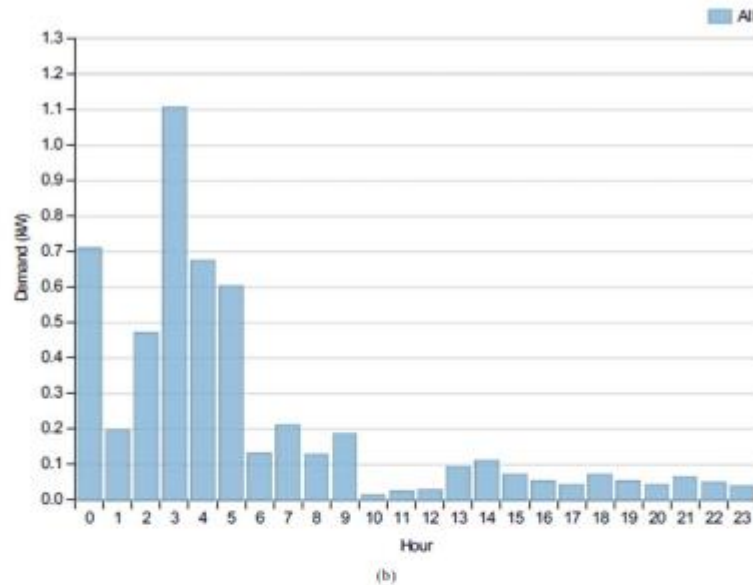


Figure 5. Load curves (a) KIST and (b) NM-AIST.

Table 5. Systems solar resources.

Quantity	KIST	NM-AIST
Sizes to consider (kW)	30, 40, 50, 70, 80	0.3, 0.4, 0.5, 0.6, 1
Lifetime	25 years	
Derating factor	80%	
Tracking system	No tracking	
Slope	6.216 degrees	3.400 degrees
Azimuth	180.000 degrees	
Ground reflectance	20.0%	

2.7. Load Demand

Demand profiles were made using year 2016 and 2017 load data sets collected during the KIST site visits. Variations in temperature were taken for the remaining months and the corresponding average load was scaled accordingly [13]. The load growth was based on sensitivity analysis in the HOMER software as shown in Table 6.

Table 6. System input load.

LOAD	KIST	NM-AIST
Data source	Synthetic	Synthetic
Daily noise	10%	10%
Hourly noise	10%	10%
Scaled annual average	851,000 kWh/d	5,167 kWh/d
Scaled peak load	60.5395 kW	1.6159 kW
Load factor	0.5857	0.1332

Once average load datasets were entered into the prototypical, variability must be introduced using HOMER's time step sensitivity capacity factor and day-to-day PV penetration functions. Appropriate values of these were determined to be 18.79% and 26.18%, respectively, in NM-

AIST and KIST 19.45% and 16.45% respectively.

2.8. System Components

Both stations were installed and each consists of several components (PV arrays, bidirectional converters and batteries for NM-AIST only). KIST was commissioned in October 2013 and expected to produce 75.63 kWp. On the other hand, NM-AIST was commissioned in July 2017 and expected to produce 0.3 kWp.

2.8.1. PV Module

PV system is employed to supply electrical power during the day from 7:15 am to 5:30 pm \pm 15 min, when there is sunshine, otherwise, battery banks take the role to supply the load in NM-AIST but in KIST there is no battery bank. In this study, all inputs are shown in Table 7.

Table 7. System inputs to PV.

Site	Size (kW)	Capital	Replacement	O&M
KIST	0.28	\$1,100.00	\$660.00	\$10.00
NM-AIST	0.15	\$600.00	\$400.00	\$10.00

2.8.2. Bidirectional Converter

Converters' size is compatible with the PV arrays for KIST and NM-AIST, the size to ensure full supply of PV power and was taken as 100kW and 1kW respectively. The capital and replacement costs of the converters are 3,000 \$/kW, 600 \$/kW and 1,800 \$/kW, 600 \$/kW respectively, while 10 \$/year and 0 \$/year are marked for operating and maintenance costs respectively. The operational lifetime was considered to be 10 years. The sizes are considered to 25.21,

40, 50.42, 75.63, 100 kW for KIST and 5 kW for NM-AIST.

2.8.3. Battery Energy Storage

Lead acid type 1 kWh of energy storage batteries is employed in NM-AIST sites, each cell is made up of 12 V, and connected as four strings, each string with a maximum capacity of 4.0 kW, 83.4 Ah and contains 4 units. The capital, replacement and operating and maintenance costs are 300 \$/kW, 300 \$/kW and 10 \$/kW respectively. KIST system has no battery storage.

2.9. Operating Strategies

Under normal operating conditions, the insolation is abundantly available and SPV control system gives the highest priority PV arrays to supply the loads. In the case of excess energy supply, the system automatically charges the battery to full capacity beyond which the excess energy is used by dumped loads. However, in case of insufficient energy from the PV system, the battery supply loads until the minimum state of charge is reached. The charging/discharging the battery happens every hour, and is based on the energy balance computations made within the system due to ultimate decision of the control system of the energy sources.

Hence, the reliable based on the amount of power supplied when PV quantity abruptly decreases and/ or the load demand suddenly increases. In this study, the operating reserve values were 15% and 22% for KIST and NM-AIST respectively of the renewable fraction that represents the fraction of the energy delivered to the load that produced from renewable power sources.

3. Results

The simulation results for the technical, economic and environmental analyses including sensitivity of the PV system configurations show that the effects of solar PV in cost, net production costs, feed-in-tariff, inverter prices, battery prices and demand growth over the years is high. The simulations from the HOMER software as well as the results for each station analysis are presented below (Sections 3.1 to 3.7) for both existing systems of implemented by HOMER.

3.1. Hourly Time Series Analysis

The hourly time series shown in Figures 6 and 7 for KIST and NM-AIST respectively.

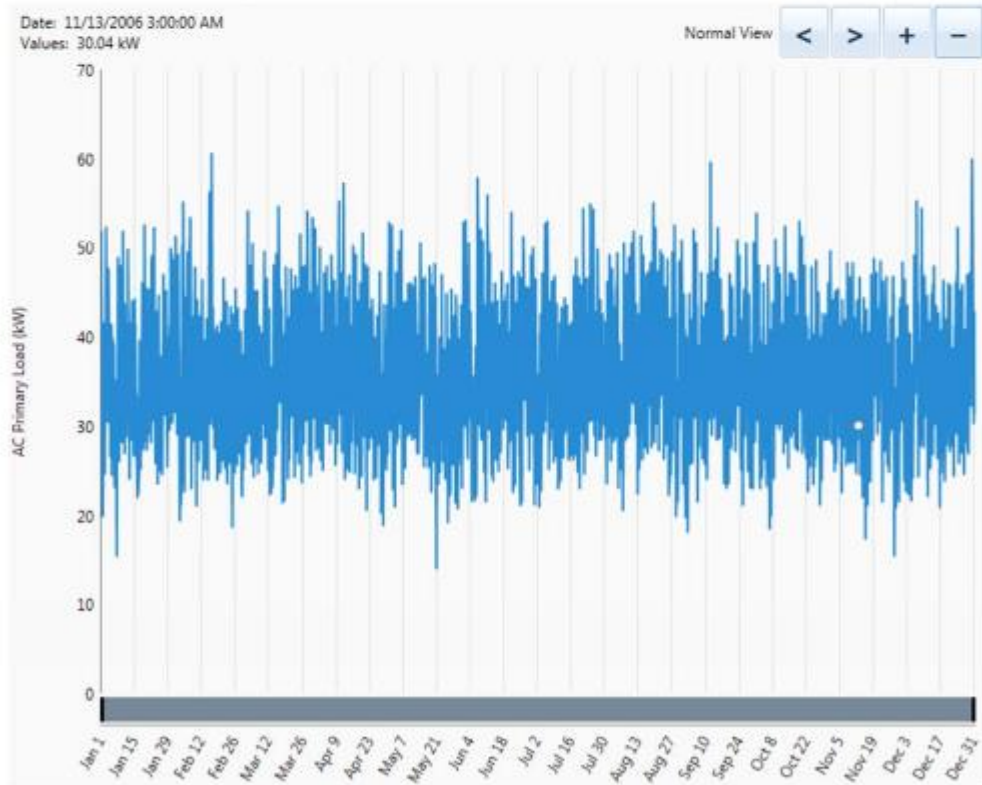


Figure 6. KIST hourly time series analysis results.

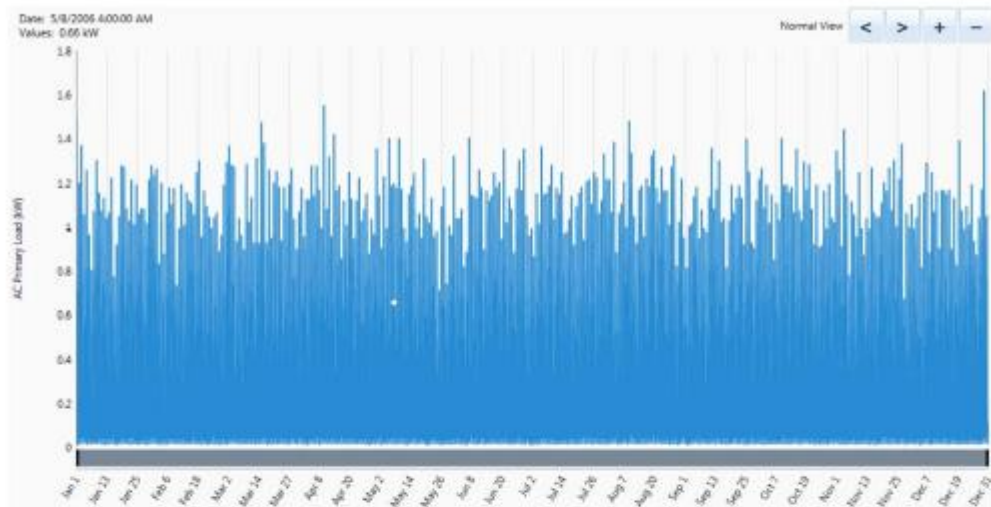


Figure 7. NM-AIST hourly time series analysis results.

3.2. Sensitivity and Optimization Cases Results

A sensitivity analysis by entering multiple values for a particular input variable, hence an input variable for which you have specified multiple values is called a sensitivity variable. The systems sensitivity are 0.3kW PV with net present cost \$29,169 and 30kW PV with net present cost \$474,475 for KIST and NM-AIST respectively. Other results are as shown in Figures 8 and 9.

3.3. Renewable Penetration

The penetration of renewable energy was compared to the amount of electricity consumed. In this context, renewable

penetration refers to the percentage of electricity generated by a particular resource as the percentage relative to the total amount of electricity generated, or the amount consumed.

3.4. Grid

In grid systems, the capital cost, the replacement cost and the fuel cost of the grid are always zero. The operating and maintenance cost is equal to the annual cost of buying electricity from the grid (energy cost plus demand cost) minus any income from the sale of electricity to the grid as shown in Figure 10 for KIST and NM-AIST respectively.

Sensitivity Cases: Left Click on sensitivity case to see optimization cases.									
Architecture					Cost				System
PV (kW)	Battery (kWh)	G (kW)	BOE LP (kW)	Dispatch	COE (\$)	NPC (\$)	Operating cost (\$)	Initial capital (\$)	Ren Frac (%)
0.3		999,999	5	CC	\$1.062	\$29,169	\$1,931	\$4,200	22
Optimization Cases: Left Double Click on simulation to examine details.									
Architecture					Cost				System
PV (kW)	Battery (kWh)	G (kW)	BOE LP (kW)	Dispatch	COE (\$)	NPC (\$)	Operating cost (\$)	Initial capital (\$)	Ren Frac (%)
0.3		999,999	5	CC	\$1.062	\$29,169	\$1,931	\$4,200	22
0.4		999,999	5	CC	\$1.000	\$29,181	\$1,901	\$4,600	28
0.5		999,999	5	CC	\$0.946	\$29,320	\$1,882	\$5,000	33
0.3	2	999,999	5	CC	\$1.074	\$29,499	\$1,945	\$4,350	22
0.4	2	999,999	5	CC	\$1.012	\$29,511	\$1,915	\$4,750	28
0.5	2	999,999	5	CC	\$0.997	\$29,531	\$1,897	\$5,400	37
0.6	2	999,999	5	CC	\$0.956	\$29,657	\$1,896	\$5,150	33
0.6	2	999,999	5	CC	\$0.907	\$29,861	\$1,881	\$5,550	37
1.0		999,999	5	CC	\$0.750	\$30,509	\$1,819	\$7,000	50
1.0	2	999,999	5	CC	\$0.759	\$30,839	\$1,832	\$7,150	50

Figure 8. NM-AIST sensitivity and optimization analysis results.

Sensitivity cases: Overall													
Architecture				Cost				System	PV		Converter		G
PV (kW)	G	Converter (kW)	Dispatch	COE (\$)	NPC (\$)	Operating Cost (\$)	Initial Capital (\$)	Ren Frac (%)	Capital Cost (\$)	Production	Rectifier Mean Output	Inverter Mean Output	Energy Produced
30	999,999	25.2	CC	\$0.118	\$474,745	\$27,548	\$118,613	15	\$117,857	51,108	0	5	264,624
Optimization case: Overall													
Architecture				Cost				System	PV		Converter		G
PV (kW)	G	Converter (kW)	Dispatch	COE (\$)	NPC (\$)	Operating Cost (\$)	Initial Capital (\$)	Ren Frac (%)	Capital Cost (\$)	Production	Rectifier Mean Output	Inverter Mean Output	Energy Produced
30	999,999	25.2	CC	\$0.118	\$474,745	\$27,548	\$118,613	15	\$117,857	51,108	0	5	264,624
30	999,999	40.0	CC	\$0.118	\$475,294	\$27,556	\$119,057	15	\$117,857	51,108	0	5	254,520
30	999,999	50.4	CC	\$0.118	\$475,665	\$27,563	\$119,370	15	\$117,857	51,108	0	5	254,520
30	999,999	75.6	CC	\$0.119	\$476,630	\$27,577	\$120,126	15	\$117,857	51,108	0	5	254,520
30	999,999	100.0	CC	\$0.119	\$477,544	\$27,581	\$120,857	15	\$117,857	51,108	0	5	254,520
40	999,999	40.0	CC	\$0.124	\$499,401	\$26,382	\$158,343	20	\$157,143	68,114	0	7	249,348
40	999,999	50.4	CC	\$0.124	\$499,792	\$26,384	\$158,633	20	\$157,143	68,114	0	7	249,348
40	999,999	75.6	CC	\$0.125	\$500,737	\$26,401	\$159,412	20	\$157,143	68,114	0	7	249,348
40	999,999	25.2	CC	\$0.125	\$501,625	\$26,589	\$157,899	19	\$157,143	68,114	0	7	252,450
40	999,999	100.0	CC	\$0.125	\$501,651	\$26,417	\$160,143	20	\$157,143	68,114	0	7	249,348
50	999,999	40.0	CC	\$0.130	\$523,827	\$25,233	\$197,629	25	\$196,429	85,100	0	9	254,696
50	999,999	75.6	CC	\$0.130	\$525,096	\$25,248	\$198,697	25	\$196,429	85,100	0	9	234,666
50	999,999	100.0	CC	\$0.133	\$526,010	\$25,263	\$199,429	25	\$196,429	85,100	0	9	242,830
50	999,999	25.2	CC	\$0.133	\$534,365	\$26,062	\$197,185	22	\$196,429	85,100	0	8	211,992
70	999,999	50.4	CC	\$0.140	\$576,503	\$21,206	\$276,513	33	\$275,000	119,252	0	12	211,972
70	999,999	75.6	CC	\$0.140	\$576,660	\$21,159	\$277,269	34	\$275,000	119,252	0	12	211,972
70	999,999	100.0	CC	\$0.140	\$577,574	\$21,173	\$278,000	34	\$275,000	119,252	0	12	213,443
70	999,999	40.0	CC	\$0.144	\$582,113	\$21,664	\$276,200	32	\$275,000	119,252	0	11	204,262
80	999,999	75.6	CC	\$0.143	\$503,994	\$22,235	\$316,555	38	\$314,286	136,288	0	14	204,262
80	999,999	100.0	CC	\$0.141	\$504,908	\$22,249	\$317,246	34	\$314,286	136,288	0	14	204,321
80	999,999	50.4	CC	\$0.145	\$506,828	\$22,512	\$315,796	37	\$314,286	136,288	0	14	252,381
70	999,999	25.2	CC	\$0.152	\$508,532	\$25,742	\$275,736	25	\$275,000	119,252	0	9	252,383
80	999,999	40.0	CC	\$0.152	\$516,309	\$21,270	\$315,436	34	\$314,286	136,288	0	12	206,568
80	999,999	100.0	CC	\$0.143	\$504,908	\$22,249	\$317,266	38	\$314,286	119,252	0	14	204,262
80	999,999	50.4	CC	\$0.143	\$506,828	\$22,512	\$315,794	37	\$314,286	136,288	0	14	204,321
70	999,999	25.2	CC	\$0.152	\$508,532	\$25,742	\$276,756	25	\$275,000	119,252	0	9	232,283
80	999,999	40.0	CC	\$0.152	\$516,309	\$21,270	\$315,446	34	\$314,286	136,288	0	12	206,509
80	999,999	25.2	CC	\$0.162	\$548,068	\$25,761	\$315,042	28	\$314,286	136,288	0	9	208,966

Figure 9. KIST sensitivity and optimization analysis results.

Month	Energy Purchased (kWh)	Energy Sold (kWh)	Net Energy Purchased (kWh)	Peak Demand (kW)	Energy Charge (\$)	Demand Charge (\$)
January	21,964	2	21,961	51	\$2,196.20	\$0
February	19,201	0	19,201	50	\$1,920.10	\$0
March	22,722	0	22,722	52	\$2,272.20	\$0
April	22,222	0	22,222	51	\$2,222.20	\$0
May	22,519	0	22,519	47	\$2,251.90	\$0
June	22,595	0	22,595	54	\$2,259.50	\$0
July	22,846	0	22,846	51	\$2,284.60	\$0
August	23,571	0	23,571	49	\$2,357.10	\$0
September	21,633	0	21,633	50	\$2,163.30	\$0
October	22,120	0	22,120	46	\$2,212.00	\$0
November	21,035	0	21,035	48	\$2,103.50	\$0
December	22,196	0	22,196	49	\$2,219.60	\$0
Annual	264,624	2	264,622	54	\$26,462.00	\$0

(a)

Month	Energy Purchased (kWh)	Energy Sold (kWh)	Net Energy Purchased (kWh)	Peak Demand (kW)	Energy Charge (\$)	Demand Charge (\$)
January	122	24	97	1	\$127.30	\$0
February	141	24	117	1	\$148.03	\$0
March	136	20	116	2	\$142.89	\$0
April	137	18	120	1	\$144.39	\$0
May	140	15	125	1	\$146.97	\$0
June	142	16	126	1	\$149.15	\$0
July	147	17	130	1	\$154.66	\$0
August	135	21	114	1	\$141.88	\$0
September	140	21	118	1	\$146.74	\$0
October	132	19	113	1	\$138.56	\$0
November	140	21	120	2	\$147.27	\$0
December	140	21	120	2	\$147.27	\$0
Annual	1,651	239	1,412	2	\$1,734.20	\$0

(b)

Figure 10. Energy operation results (a) KIST and (b) NM-AIST.

3.5. System Converter

The results of the systems converters are as shown in Figures 11 and 12 for KIST and NM-AIST respectively

Quantity	Inverter	Rectifier	Units	Quantity	Inverter	Rectifier	Units
Capacity	25.20	22.68	kW	Hours of Operation	4,338.00	0.00	hrs/yr
Mean Output	5.25	0.00	kW	Energy Out	45,993.00	0.00	kWh/yr
Minimum Output	0.00	0.00	kW	Energy In	51,103.00	0.00	kWh/yr
Maximum Output	25.21	0.00	kW	Losses	5,110.20	0.00	kWh/yr
Capacity Factor	20.83	0.00	%				

Figure 11. KIST – System inverter/converter results.

Quantity	Inverter	Rectifier	Units	Quantity	Inverter	Rectifier	Units
Capacity	5.00	4.80	kW	Hours of Operation	4,326.00	0.00	hrs/yr
Mean Output	0.05	0.00	kW	Energy Out	474.04	0.00	kWh/yr
Minimum Output	0.00	0.00	kW	Energy In	493.80	0.00	kWh/yr
Maximum Output	0.28	0.00	kW	Losses	19.75	0.00	kWh/yr
Capacity Factor	1.08	0.00	%				

Figure 12. NM-AIST – system inverter/converter results.

3.6. NM-AIST Storage Battery

The results of the NM-AIST storage battery shows that autonomy 5.57 hours, other results are as shown in Figures 13.

Quantity	Value	Units	Quantity	Value	Units	Quantity	Value	Units
String Size	2.00		Nominal Capacity	2.00	kWh	Energy In	1.34	kWh/yr
Strings in Parallel	1.00		Usable Nominal Capacity	1.20	kWh	Energy Out	1.07	kWh/yr
Batteries	2.00		Autonomy	5.57	hr	Storage Depletion	0.00	kWh/yr
Bus Voltage	24.00	V	Lifetime Throughput	1,600.00	kWh	Losses	0.27	kWh/yr
			Battery Wear Cost	0.10	\$/kWh	Annual Throughput	1.20	kWh/yr
			Average Energy Cost	1.05	\$/kWh	Expected Life	10.00	yr

Figure 13. NM-AIST storage battery results.

3.7. Emission

The emissions results suggest that the total amount of each pollutants produced per annum by the existing power system are relatively small to cause emissions with KIST emitting

more greenhouse gases than NM-AIST. The major greenhouse gas pollutants include carbon dioxide, carbon monoxide, unburned hydrocarbons and particulate matter, sulfur dioxide, and nitrogen oxides (Figure 14). Therefore,

sales of power to the grid result in reduced grid emissions.

Quantity	Value	Units
Carbon Dioxide	167,241.00	kg/yr
Carbon Monoxide	0.00	kg/yr
Unburned Hydrocarbons	0.00	kg/yr
Particulate Matter	0.00	kg/yr
Sulfur Dioxide	725.06	kg/yr
Nitrogen Oxides	354.59	kg/yr

(a)

Quantity	Value	Units
Carbon Dioxide	892.29	kg/yr
Carbon Monoxide	0.00	kg/yr
Unburned Hydrocarbons	0.00	kg/yr
Particulate Matter	0.00	kg/yr
Sulfur Dioxide	3.87	kg/yr
Nitrogen Oxides	1.89	kg/yr

(b)

Figure 14. Energy emission (a) KIST and (b): NM-AIST.

4. Conclusion

This study shows that solar photovoltaics (SPV) systems should be considered as a renewable alternative energy source with high output performance in any simulated supply plan. The simulation results from the HOMER software indicate that PV is efficient.

The economic analysis of the PV systems showed a low net present cost (NPC) relative to the break-even grid extension distance from the simulated system locations in both NM-ASIT and KIST. However, when the systems were connected to the external grid, the most economically feasible options were feasible because there was no capital costs involved while the operation and maintenance costs were much less compared to the grid system only. In brief, the integration of the solar PV systems presents one of the most environmentally friendly energy options to mitigate greenhouse gas emissions, which simultaneously save against the high initial capital and replacement costs involved with hydroelectric on the grid systems.

References

- [1] Gwang'ombe, F. and N. Mwiha, Renewable in Tanzania: Status and Prospects of Biomass Based Cogeneration and Geothermal Technologies. HBF-HA, Sida/SAREC and AFREPREN/FWD, 2005.
- [2] Kassenga, G., The status and constraints of solar photovoltaic energy development in Tanzania. *Energy Sources, Part B*, 2008. 3 (4): p. 420-432.
- [3] Hoffmann, C., E. Romero, and E. Alonso, Combining different controlled-suction techniques to study expansive clays. in *Proceedings of the international symposium on advanced experimental unsaturated soils mechanics EXPERUS*, Trento, Balkema, 2005.
- [4] Hoffmann, W., PV solar electricity industry: Market growth and perspective. *Solar energy materials and solar cells*, 2006. 90 (18): p. 3285-3311.
- [5] Lillenthal, P., HOMER® micropower optimization model, 2005, National Renewable Energy Laboratory (NREL), Golden, CO.
- [6] Liu, G., et al., Techno-economic simulation and optimization of residential grid-connected PV system for the Queensland climate. *Renewable Energy*, 2012. 45: p. 146-155.
- [7] Bernal-Agustin, J. L. and R. Dufo-Lopez, Simulation and optimization of stand-alone hybrid renewable energy systems. *Renewable and Sustainable Energy Reviews*, 2009. 13 (8): p. 2111-2118.
- [8] Anwar, M., et al. Photovoltaic power system simulation for small industry area. in *Electrical, Control and Computer Engineering (INECCE)*, 2011 International Conference on. 2011. IEEE.
- [9] Ani, V. A. and B. Abubakar, Feasibility Analysis and Simulation of Integrated Renewable Energy System for Power Generation: A Hypothetical Study of Rural Health Clinic. *Journal of Energy*, 2015. 2015.
- [10] González, P., et al. Impact of Grid Connected Photovoltaic System in the Power Quality of a Distribution Network. in *DoCEIS*. 2011. Springer.
- [11] Khatib, T., A. Mohamed, and K. Sopian, A software tool for optimal sizing of PV systems in Malaysia. *Modelling and Simulation in Engineering*, 2012. 2012: p. 10.
- [12] Klein, S., Calculation of monthly average insolation on tilted surfaces. *Solar energy*, 1977. 19 (4): p. 325-329.
- [13] Mishra, S., C. Panigrahi, and D. Kothari, Design and simulation of a solar-wind-biogas hybrid system architecture using HOMER in India. *International Journal of Ambient Energy*, 2016. 37 (2): p. 184-191.

Output 2: Poster presentation

